Energy xxx (xxxx) xxx

Contents lists available at ScienceDirect

Energy

journal homepage: www.elsevier.com/locate/energy

Optimal sizing and power schedule in PV household-prosumers for improving PV self-consumption and providing frequency containment reserve

M. Gomez-Gonzalez [a], J.C. Hernandez [b, *], D. Vera [a], F. Jurado [a]

[a] Department of Electrical Engineering, University of Jaén, Escuela Politécnica Superior, 23700, Linares, Jaén, Spain
[b] Department of Electrical Engineering, University of Jaén, Campus Lagunillas s/n, Edificio A3, 23071, Jaén, Spain

ARTICLE INFO

Article history:
Received 3 July 2019
Received in revised form
4 November 2019
Accepted 14 November 2019
Available online xxx

Keywords:
Batteries
Electric vehicle
Frequency containment reserve
Lifetime
Power management strategy
PV power systems

ABSTRACT

This paper presents a methodology for jointly optimizing the sizing and power management of PV household-prosumers, namely, photovoltaic (PV) power, electric vehicle charging load (EVCL), household consumption load (HCL), battery bank (BB), and power converters. The optimization includes PV self-consumption enhancement and frequency containment reserve (FCR). This innovative model uses an annual techno-economic assessment to calculate the total costs and revenue by means of the teaching-learning-based optimization (TLBO) algorithm. The assessment of BB aging takes into account the charge/discharge power as well as the depth of discharge (DOD). This methodology is applied to Spanish PV household-prosumers. Results are obtained for scenarios involving PV, EV, and BB. Moreover, the PV household-prosumer approximated the smart user concept by providing FCR service. The scenarios envisaged examined potential revenues based on markets (day-ahead and FCR market) and their influence on profitability. The results of this study confirmed that BB is a cost-effective way of enhancing PV self-consumption by decreasing the levelized cost of electricity (LCOE). In fact, when FCR provision was added, there was a significant increase in the total revenue with a relatively low impact on BB aging.
© 2019 Elsevier Ltd. All rights reserved.

1. Introduction

Within distribution networks, the integration of more PV household-prosumers (i.e., a converter-based distributed generation [CbDG]) is a visible trend [1]. Without netting arrangements, these prosumers must increase their PV self-consumption for economic reasons, and BB attachment is the most effective way of accomplishing this [2–11]. Furthermore, they can provide balancing services [12–15] and trade on the day-ahead market to maximize their benefit [2,16].

Greater penetration of CbDG in power systems would reduce the inertia and frequency control reserve [17–20]. Consequently, to ensure transient stability in power systems, the latest network codes and standards in the European Union [21–27] advise or require CbDG to synthetically inherit balancing service functions from conventional generation and then to provide them. In a future smart-grid scenario [28], PV household-prosumers would be able to receive operation references from an aggregator. These would mainly be active and reactive power commands for delivering balancing services [29,30]. In comparison to other balancing services, FCR is suitable for battery-based PV household-prosumers [20,31,32].

Balancing services require high power and energy installations, ranging from 100 kW to an order of MW [12,33,34]. However, this fact may no longer be an impediment for the massive deployment of PV household-prosumers-providing services since the figure of the aggregator agent using CbDG and/or energy storage system (ESS) is expanded [31,35–38]. The aggregator is a stakeholder balances service markets and shares their service provision duties among smart users. In the future, most smart PV household-prosumers will be able to manage renewable powers [39] and ESSs [40].

References [12–15] found a substantial increase in the profitability of PV-battery systems when PV self-consumption enhancement was combined with the provision of FCR or frequency regulation reserves (FRR). Other studies demonstrated the techno-economic feasibility of providing FCR by EVs [18,41,42] or

* Corresponding author.
E-mail addresses: mggonzal@ujaen.es (M. Gomez-Gonzalez), jcasa@ujaen.es (J.C. Hernandez), dvera@ujaen.es (D. Vera), fjurado@ujaen.es (F. Jurado).

https://doi.org/10.1016/j.energy.2019.116554
0360-5442/© 2019 Elsevier Ltd. All rights reserved.

Please cite this article as: Gomez-Gonzalez M et al., Optimal sizing and power schedule in PV household-prosumers for improving PV self-consumption and providing frequency containment reserve, Energy, https://doi.org/10.1016/j.energy.2019.116554

Nomenclature

List of symbols

Δ_t discretization time period [0.5 h]
ε_{uB} MBU self-discharge coefficient [%/hour]
η_{ad} AC/DC converter efficiency [%]
θ_{ub} fraction of life consumed or cumulated aging rate of an MBU [p.u.]
κ_k ratio of operation and maintenance cost vs. initial investment cost for the kth HMG component [%]
λ^a_{ub} number of cycles per year of an MBU [cycles/year]
$\lambda^{\max}_{ub}$ maximum number of cycles over the MBU lifetime [cycles]
ξ^j_{fcr-} and ξ^j_{fcr+} per-unit downward- and upward-FCR power availability at any time period j at the Spanish level (base power: annual maximum FCR power) [p.u.]
ξ^j_{pv} per-unit PV power output at any time period j of an MPVU (base power: P_{upv}) [p.u.]
ρ^j_{RTPEP} / ρ^j_{RTSEP} real-time purchasing/selling energy price at any time period j in the respective real-time pricing scenario [€/kWh]
ρ^j_{RTPPAP} / ρ^j_{RTSPAP} real-time purchasing/selling power availability price at any time period (capacity charge of the FCR [€/kW]
ρ^j_{RTPEUP} / ρ^j_{RTSEUP} real-time purchasing/selling energy utilization price at any time period j (energy charge of the FCR) [€/kWh]
χ^{rat}_{ub} rated DOD of an MBU [%]
Ω_{uad} number of MADUs installed in the AC/DC converter
$a_i \quad \forall_i$ coefficients
$C^a_{hmg} = \text{NPV}^a_{hmg}$ total annual cost (or annual NPV) of HMG [€/year]
$C^a_{EE,hmg}(C^j_{EE,hmg})$ annual (at any time period j) net income from energy exchange of the HMG with the LV AC grid [€/year], ([€/period])
$\{C^a_{I,hmg,k}\}(C^a_{O\&M,hmg,k})$ $[C^a_{R,hmg,k}]$ total annual cost {initial investment}(operation and maintenance) [replacement] for the kth HMG component [€/year]
$C_{O\&M,hmg,k}$ operation and maintenance for the kth HMG component [€/year]
$C^a_{FCR,hmg}(C^j_{FCR,hmg})$ annual (at any time period j) net income from FCR provision of the HMG to the LV AC grid [€/year], ([€/period])
$(C^a_{uad})C_{uad}$ (annual) cost of an MADU ([€/year]), [€/unit]
$(C^a_{ub})C_{ub}$ (annual) cost of an MBU ([€/year]), [€/unit]
$(C^a_{upv})C_{upv}$ (annual) cost of an MPVU ([€/year]), [€/unit]
d nominal discount rate [%]
DoD death of discharge [%]
$E^j_{\text{fcr}-}$ and $E^j_{\text{fcr}+}(E^j_{\text{ufcr}-}$ and $E^j_{\text{ufcr}+})$ cumulated stored and released FCR energy in the HMG (MFCRU) at any time period j [kWh]
g inflation rate [%]
k index kth of HMG component (PV, battery, AC/DC converter)
Le^{beg}_{ub} beginning energy of MBU [kWh]
Le^{end}_{uB} end energy of MBU [kWh]
$Le^{\max}_{ub}$ maximum energy of MBU [kWh]
$LCOE_{hmg}$ levelized cost of energy for the HMG [€/kWh]
m index of cycle among all the cycles
N_c all discharge cycles [cycles]
N_{uad} MADU lifetime [years]
N_{ub} MBU lifetime [years]
$N_{\theta^{\max}_{ub}}$ MBU lifetime according to maximum cumulated aging rate [years]
N_{upv} MPVU lifetime [years]
N_{hmg} HMG lifetime [years]
P_c contracted power from the electric mains [kW]
$P^{\max}_{ub-}$ / $P^{\max}_{ub+}$ maximum charge/discharge power for an MBU [kW]
P_{ufcr} prequalified power capacity of an MFCRU [kW]
P_{uad} rated power of an MADU [kW]
P_{upv} rated power of an MPVU [kW]
p^j_{ev} EVCL at any time period j [kW]
p^j_{hl} HLC at any time period j [kW]
p^j_{pv} / p^j_{upv} PV power output in the HMG/MPVU at any time period j [kW]
$p^j_{\text{fcr}-}$ and $p^j_{\text{fcr}+}(p^j_{\text{ufcr}-}$ and $p^j_{\text{ufcr}+})$ downward- and upward-FCR power activation in the HMG (MFCRU) at any time period j [kW]
$p^j_{g-}(p^j_{g+})$ grid power output(input) at any time period j [kW]
$r_{O\&M}$ annual escalation rate of the operation and maintenance cost [%]
r_{pv} PV degradation rate [%]
t time
T income tax rate [%]

control variables

$\boldsymbol{p^j_{b-}}$ / $\boldsymbol{p^j_{b+}}$ [1] charge/discharge power of the BB at any time period j [kW][11]
$\boldsymbol{\Omega_{ub}}$ number of MBUs installed in the BB
$\boldsymbol{\Omega_{upv}}$ number of MPVUs installed in the PV system
$\boldsymbol{\Omega_{ufcr}}$ number of MFCRU

state variables

Le^j_b BB energy at any time period j [kWh]
$Le^{\max,j}_b$ maximum BB energy at any time period j [kWh]
$Le^{\min,j}_b$ minimum BB energy at any time period j [kWh]

Subscripts

ad AC/DC converter
b-/b+ to the battery/from the battery
ev EVCL
EE energy exchange with the LV AC grid
FCR FCR
FCR+/FCR FCR to the LV AC grid (upward regulation)/FCR from the LV AC grid (downward regulation)
g-/g+ to the grid/from the grid
hl HLC
hmg HMG
I initial investment

Please cite this article as: Gomez-Gonzalez M et al., Optimal sizing and power schedule in PV household-prosumers for improving PV self-consumption and providing frequency containment reserve, Energy, https://doi.org/10.1016/j.energy.2019.116554

max	maximum
min	minimum
O&M	operation and maintenance
pv	photovoltaic
R	replacement
u	to refer to minimum unit

Superscripts

a	annual
beg	at the beginning
end	at the end
j	index of time period
max	maximum
min	minimum
rat	rated

Abbreviations

BB	battery bank
BSP	balancing service provider
CbDG	converter-based distributed generation
DOD	death of discharge
ESS	energy storage system
EV	electric vehicle
EVCL	EV charging load
FCR	frequency containment reserve
FMS	frequency management system
FRR	frequency regulation reserve
HLC	household consumption load
HMG	household microgrid
LCOE	levelized cost of energy
MADU	minimum AC/DC converter unit
MBU	minimum battery unit
MFCRU	minimum FCR unit
MPVU	minimum PV unit
NPV	net present value
PSO	particle swarm optimization
PV	photovoltaic
SO	system operator
SOC	state of charge
TLBO	teaching-learning-based optimization
UCTE	union for the co-ordination of transmission of electricity

battery ESSs [20,32,43–46]. Maintaining the state of charge (SOC) of ESSs was analyzed to ensure continuous FCR availability [12,18,47,48]. Other papers discussed battery aging when providing FCR [49–51]. However in households, the sizing optimization of PV-battery systems has only encompassed PV self-consumption systems [1,4–11,52]. Nonetheless, different optimization techniques have been applied to optimally size batteries and/or renewable power in microgrids and thus maximize economic benefits [53–60].

Certain studies developed optimization techniques for determining the optimal power management and sizing of battery-based microgrids with a view to providing balancing services [37,61,62]. However, optimal power management in ESSs for grid-connected systems has been studied somewhat less frequently. References [16,63–67] formulated and solved optimization techniques for this type of ESS power management. Previous optimization formulations were usually applied on a punctual [54] or daily basis [16,37,53,58,59,61,63–67]. Only a few studies envisaged longer horizons such as various days [60], one month [62], one year [55,56], or several years [57]. The concept of providing FCR and enhancing PV self-consumption based on hybrid ESSs has recently gained attention in the literature [68–70].

The primary contribution of this paper is a methodology that addresses PV self-consumption enhancement and FCR provision for the joint optimization of the power management and sizing of PV household-prosumers. For this purpose, an innovative model was devised, which is able to calculate associated total costs and revenues by means of an annual techno-economic assessment, which takes into account a representative set of days. Costs and revenues include investment, operation and maintenance, replacement, net income from the energy exchange, and FCR provision. The technique used for solving the optimization problem is the teaching-learning-based optimization (TLBO) algorithm [71,72]. Also it was presented is a way to accurately model battery aging. This new methodology was applied to a case study of Spanish PV household-prosumers, based on current FCR data in Spain. When FCR data were not available, data from the European balancing services market were used.

Despite the potential value of this approach, its long-term economic implications have not as yet been studied in any depth. This research is thus a key contribution to sizing and power management since it takes into account the real economic advantage of PV self-consumption enhancement combined with FCR provision while also considering battery aging. However, one of the weaknesses of this methodology is that it does not account for the newest way of providing FCR and enhancing PV self-consumption based on hybrid ESSs. Another limiting factor is that a high optimization resolution of 30 min cannot fully capture either the fast frequency response or the effects of high frequency input cycling on large deviations in temperature, charge/discharge power rate and DOD for the BB [70,73]. This is important in the evaluation of battery degradation due to the fast grid service of FCR or the PV self-consumption enhancement [62,70,74].

The remainder of this paper is structured as follows: Section 2 describes the PV household-prosumer. Section 3 gives a brief overview of European balancing service markets. Section 4 describes the optimization methodology and how it solves sizing and power management. Section 5 shows the input data sets required for this purpose. Section 6 presents the results and analysis of the Spanish case study in which different scenarios are contemplated. Finally, Section 7 summarizes the conclusions that can be derived from this research and describes plans for future work.

2. The PV household-prosumer

This paper analyzes a PV household-prosumer, hereafter called household microgrid (HMG), consisting of a PV system, EVCL, HLC, BB, and AC/DC power converter, Fig. 1. The HMG is connected to the LV AC grid to inject/abort power and provide FCR. The energy and power directions are used as a reference throughout the paper. The PV system and BB are the primary energy sources to cover the loads, whereas the LV AC grid is used as a backup.

3. European balancing service market

The balancing market is the institutional arrangement that deals with the balancing of electricity demand and supply in an unbundled electricity market [75]. This market consists of three main phases: balance planning, balancing service provision, and balance settlement [35].

There are two main types of balancing service: (i) balancing

[1] Control variables are shown in bold letters.

Please cite this article as: Gomez-Gonzalez M et al., Optimal sizing and power schedule in PV household-prosumers for improving PV self-consumption and providing frequency containment reserve, Energy, https://doi.org/10.1016/j.energy.2019.116554

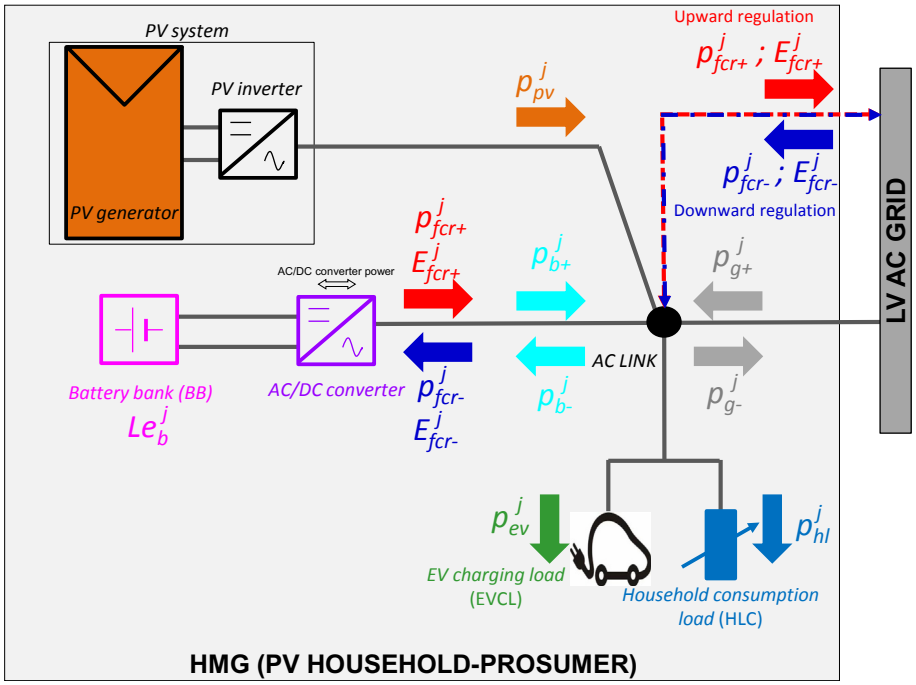

Fig. 1. Set-up of the HMG.

energy, which is the real-time adjustment of balancing resources of a balancing service provider (BSP) to maintain the system balance [76]; (ii) balancing capacity, which is a volume of reserve capacity that a BSP has agreed to hold and in respect to which has agreed to submit bids for a corresponding volume of balancing energy for the duration of the contract [76]. Furthermore, one can also differentiate between upward and downward regulation.

The main classes of balancing service are FCR, FRR, and replacement reserves. Each one has a different function and set of technical requirements for entering its unbundled market [77]. FCR service is the first reserve activated. The aim is not to re-establish the frequency at the desired level but only to respond very quickly to disturbances. It is a decentralized automatic service, which is continuously activated, and whose response is provided in a matter of seconds.

3.1. Technical requirements for entering in FCR market

Technical requirements for entering balancing markets are very strict and depend on the type of balancing service [78,79]. Despite incentives in European Directives to open markets for aggregator agents [36], only a few countries (e.g. Scandinavian countries, UK, France, Germany, and Belgium) have done this so far, though always with specific technical requirements, based on the following: minimum bid size, product resolution, symmetry of the offer, and duration of the activation.

Reference [80] summarizes the technical requirements for providing FCR with large generators connected to the system of Union for the Co-ordination of Transmission of Electricity (UCTE). Nonetheless, system operators (SOs) have recently introduced [81] specific technical requirements for CbDG connected to MV [21–24] and LV [25–27] grids that strongly advise FCR provision [21–27]. Since the HMG proposed in this research is covered by these new regulations, it can provide FCR, according to standards.

3.2. Economic features of FCR market

Balancing services are provided by BSPs [79] to the SO by bidding in balancing service markets. Nonetheless, SO in particular can acquire FCR through compulsory provision, bilateral tendering, and the spot market. The economic features of the balancing service market are summarized in Ref. [32]. Accordingly, the pricing mechanisms used for the settlement of selected bids can be one of the following: regulated prices, pay-as-bid pricing, marginal pricing, or common clearing price. The preferred FCR remuneration method is marginal pricing [35]. This includes an availability payment and an additional amount for utilization.

4. Optimization methodology

4.1. Optimization technique

The methodology for jointly optimizing the sizing and power management of PV household-prosumers should depend on the nature of the problem (i.e. technical and financial indicators, control variables, and constraints). This is regarded as a constrained problem with a finite horizon (one year). In addition, all input disturbances are assumed to be deterministic. These include PV power, HLC, EVCL, FCR data, and the energy price. The control variables are continuous, and the constraints and objective function are not particularly derivable or linear. As explained in Appendix A, the TLBO algorithm is proposed as the most suitable optimization technique for the problem.

4.2. Objective function

From a technical point of view, our model supplies HCL/EVCL and provides FCR. From an economic perspective, it optimally sizes each HMG component and determines the BB power schedule by minimizing the objective function. The approach determines the time value of money by applying a discount rate. Financial indicators for the HMG are the net present value (NPV) on an annual

Please cite this article as: Gomez-Gonzalez M et al., Optimal sizing and power schedule in PV household-prosumers for improving PV self-consumption and providing frequency containment reserve, Energy, https://doi.org/10.1016/j.energy.2019.116554

basis (NPV^a_{hmg}) and the levelized cost of electricity. $LCOE_{hmg}$

Regarding HMG sizing, the model optimizes the following control variables: (i) number of minimum PV units (MPVUs) ($\boldsymbol{\Omega_{upv}}$), i.e. PV power; (ii) number of MBUs ($\boldsymbol{\Omega_{ub}}$), i.e. BB; (iii) number of MFCRUs ($\boldsymbol{\Omega_{ufcr}}$), i.e. prequalified FCR power capacity. Moreover, there is a set number of MADUs Ω_{uad}. Regarding HMG power management, the charge and discharge powers of the BB (p^j_{g-} and p^j_{g+}) are optimally scheduled.

The formulation of the deterministic multi-period optimization problem with a single objective in the time horizon under study is shown in (1)–(36). It comprises the objective function (1), economic constraints (3)–(14), and technical constraints (15)–(36).

The total annual cost of this HMG (annual NPV), which is the objective function to be minimized (1), includes five economic components: initial investment, operation and maintenance, replacement, net income from energy exchange, and net income from FCR provision.

$$\min NPV^a_{hmg} = \min C^a_{hmg} = \sum_{k\in\{pv,b,ad\}} C^a_{I,hmg,k} + \sum_{k\in\{pv,b,ad\}} C^a_{O\&M,hmg,k} + \sum_{k\in\{b\}} C^a_{R,hmg,k} + C^a_{EE,hmg} - C^a_{FCR,hmg} \tag{1}$$

When the annuitizing method is used, the levelized cost of energy (LCOE) for the HMG is defined as an economic assessment of the average total cost to build and operate this power-generating asset over its lifetime divided by its total energy consumption [82]:

$$LCOE_{hmg} = \frac{C^a_{hmg}}{\sum_{j=1}^{j=12*7*24*2}\left(p^j_{hl-} + p^j_{ev-}\right)} \tag{2}$$

4.3. Economic system modelling

The life cycle cost of the HMG can be calculated [83] by adding[2] its initial investment cost to the current value of its operation and maintenance cost, replacement cost, and net income from energy exchange, and from FCR provision over the HMG lifetime.

4.3.1. Initial investment cost

The estimated cost of the initial investment is based on data such as BB cost per installed kWh [31,32,83,84], PV cost per installed peak kW [45], and AC/DC converter cost per installed kW [45]. Accordingly, the total annual cost of the initial investment for the BB, PV system, and AC/DC converter on an annual basis is respectively:

$$C^a_{I,hmg,b} = \boldsymbol{\Omega_{ub}}\cdot C^a_{ub} = \boldsymbol{\Omega_{ub}}\cdot\frac{C_{ub}}{N_{ub}} \tag{3}$$

$$C^a_{I,hmg,pv} = \boldsymbol{\Omega_{upv}}\cdot C^a_{upv} = \boldsymbol{\Omega_{upv}}\cdot\frac{C_{upv}}{N_{upv}} \tag{4}$$

$$C^a_{I,hmg,ad} = \boldsymbol{\Omega_{uad}}\cdot C^a_{\boldsymbol{uad}} = \boldsymbol{\Omega_{uad}}\cdot\frac{C_{uad}}{N_{uad}} \tag{5}$$

4.3.2. Operation and maintenance cost

The present value of the operation and maintenance cost for the kth HMG component is:

$$C^a_{O\&M,hmg,k} = \frac{1}{N_{hmg}}\cdot C_{O\&M,hmg,k}\cdot(1-T)\cdot\frac{K_p\left(1-K_p^{N_{hmg}}\right)}{1-K_p} =;\ k\in\{pv,b,ad\} \tag{6}$$

where:

$$K_p = \frac{1+r_{O\&M}}{1+d} \tag{7}$$

$$C_{O\&M,hmg,k} = \kappa_k\cdot N_{hmg}\cdot C^a_{I,hmg,k} \tag{8}$$

4.3.3. Replacement cost

Since battery lifetime is usually less than that of the HMG, an additional investment is needed for replacement during the service life of the HMG project. The BB may reach the end of its useful life in two ways. It may either reach a maximum number of years since installation N_{ub} (calendar lifetime), or have a maximum cumulated aging rate ($\theta_{ub} = \theta^{\max}_{ub}$) at year $N_{\theta^{\max}_{ub}}$ (cycling lifetime), before reaching its maximum number of years ($N_{\theta^{\max}_{ub}} < N_{ub}$). An explanation of battery lifetime modelling is given in Appendix B. When a BB replacement is required, its annual value is:

$$C^a_{R,hmg,b} = \frac{1}{(1+d)^{\min\left(N_{\theta^{\max}_{ub}},\ N_{ub}\right)}}\cdot C^a_{I,hmg,b} \tag{9}$$

4.4. Net income from energy exchange

The net income from HMG energy exchange with the LV AC grid, due to the power balance constraint during any time period j is:

$$C^a_{EE,hmg} = \begin{Bmatrix} \rho^j_{RTPEP}\cdot\Delta_t\cdot p^j_{g+} & p^j_g \geq 0 \\ \rho^j_{RTSEP}\cdot\Delta_t\cdot p^j_{g-} & p^j_g < 0 \end{Bmatrix} \tag{10}$$

Since the price on the real-time energy market is assumed to be constant during 2018, the annual net income from energy exchange is:

$$C^a_{EE,hmg} = \frac{1}{N_{hmg}}\cdot\sum_{n=1}^{n=N_{hmg}}\frac{1}{(1+d)^n}\cdot\sum_{j=1}^{j=12*7*24*2} C^j_{EE,hmg} = \frac{q\cdot\left(1-q^{N_{hmg}}\right)}{N_{hmg}\cdot(1-q)}\cdot\sum_{j=1}^{j=12*7*24*2} C^j_{EE,hmg} \tag{11}$$

where:

$$q = \frac{1}{1+d} \tag{12}$$

[2] Unless explicitly stated otherwise, these costs hereafter are expressed on an annual basis.

4.4.1. Net income from FCR provision

BSPs who provide upward regulation receive either the upward regulation price if marginal pricing is used, or the bid price if it is a case of pay-as-bid pricing. BSPs that provide downward regulation pay the downward regulation price or the bid price [35]. BSPs with a shortage of supply vis-à-vis their nomination, pay the short imbalance settlement price for each MWh of deviation. When there is a surplus, they receive the long imbalance settlement price [85]. As HMG sizing is optimized to provide the full prequalified FCR power, the penalizations are not considered.

The HMG net income accounts for 80% of the aggregator's gain that is given to their household-prosumers [31]. The cash flow from FCR provision (power and energy buying/selling) ($C^j_{FCR,hmg}$) for any time period j is given by a first term of downward and upward FCR power availability, and a second term of upward and downward FCR energy utilization:

$$C^j_{FCR,hmg} = 0.8 * \Big[\times \left(\rho^j_{RTPPAP} \cdot p^j_{\mathrm{fcr}-} + \rho^j_{RTSPAP} \cdot p^j_{\mathrm{fcr}+} \right) + \left(\rho^j_{RTSEUP} \cdot E^j_{\mathrm{fcr}+} - \rho^j_{RTPEUP} \cdot E^j_{\mathrm{fcr}-} \right) \times \Big] \tag{13}$$

The present annual net income from FCR provision is:

$$C^a_{FCR,hmg} = \frac{1}{N_{hmg}} \cdot \sum_{n=1}^{n=N_{hmg}} \frac{1}{(1+d)} \cdot \sum_{j=1}^{j=12*7*24*2} C^a_{FCR,hmg} = \frac{q \cdot (1-q^{N_{hmg}})}{N_{hmg} \cdot (1-q)} \cdot \sum_{j=1}^{j=12*7*24*2} C^j_{FCR,hmg} \tag{14}$$

4.5. Physical system modelling

4.5.1. Technical assessment of the FCR provision from the HMG

The design of an FMS for assessing FCR power activation, based on a power-frequency characteristic [86], was previously modeled by the authors for PV-battery systems [18] and EVs [19]. This research study thus adapted the model in Refs. [18,19] to a new context. It disabled PV power in Ref. [18] and bidirectional charging in Ref. [19], and only maintained the FMS in charge of providing FCR (see Fig. 2). The FMS includes both droop and inertial response. As a result, the adapted model, which is scaled at the prequalified power capacity (P_{ufcr}) of a minimum FCR unit (MFCRU), computes the FCR power activation on a 10^{-3}-s basis [$p_{ufcr-}(t)$ and $p_{ufcr+}(t)$]. Then, the cumulated stored and released FCR energy from the HMG was evaluated by the integral of the FCR power activation during 30-min time periods. This permitted the assessment of the cumulated stored and released FCR energy (E^j_{ufrc-} and E^j_{ufrc+}) during any time period j for an MFCRU.

Technical requirements in Refs. [18,19] fulfill the requirements in Section 3.1 and the specific requirements and principles of the ENTSO-E network code [87].

4.5.2. PV power model

A simplified expression of PV power output in the HMG for any time period j is:

$$p^j_{pv} = \boldsymbol{\Omega_{upvc}} \cdot p^j_{upv} = \boldsymbol{\Omega_{upv}} \cdot \xi^j_{\mathrm{pv}} \cdot P_{upv}; \quad \forall j \tag{15}$$

The per-unit PV power output (ξ^j_{pv}) is a function of the irradiance, ambient temperature, and PV system efficiency [88].

4.5.3. Power and energy model for FCR

The upward and downward FCR power activations in the HMG for any time period j are:

$$\begin{aligned} p^j_{\mathrm{fcr}-} &= \boldsymbol{\Omega_{ufcr}} \cdot p^j_{\mathrm{ufcr}-} = \boldsymbol{\Omega_{ufcr}} \cdot \xi^j_{\mathrm{fcr}-} \cdot P_{\mathrm{ufcr}} \\ p^j_{\mathrm{fcr}+} &= \boldsymbol{\Omega_{ufcr}} \cdot p^j_{upfc+} = \boldsymbol{\Omega_{ufcr}} \cdot \xi^j_{\mathrm{fcr}+} \cdot P_{\mathrm{ufcr}} \quad \forall j \end{aligned} \tag{16}$$

The cumulated stored and released FCR energies in the HMG are:

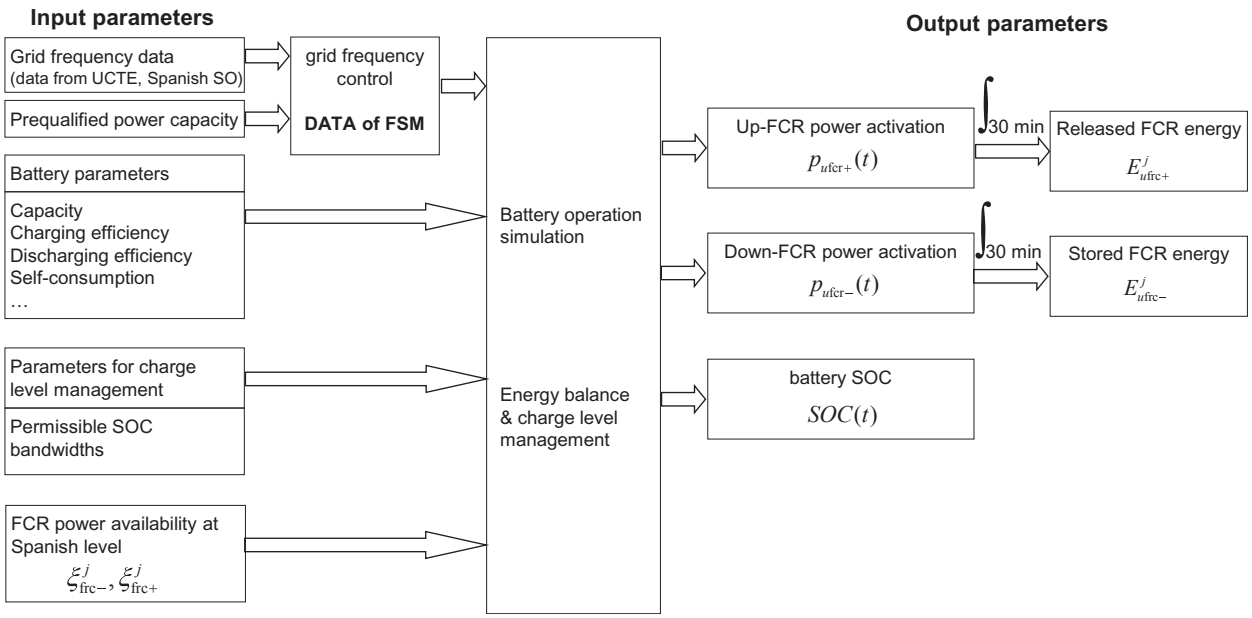

Fig. 2. Model for assessing the FCR power activation [18,19] and cumulated FCR energy.

$$E^j_{\text{fcr}-} = \boldsymbol{\Omega_{ufcr}} \cdot \xi^j_{\text{fcr}-} \cdot E^j_{\text{ufcr}-}$$
$$E^j_{\text{fcr}+} = \boldsymbol{\Omega_{ufcr}} \cdot \xi^j_{\text{fcr}+} \cdot E^j_{\text{ufcr}+} \quad \forall j \tag{17}$$

4.5.4. Battery energy model

An AC-to-DC conversion is necessary when charging the BB, and a DC-to-AC conversion is required when the BB is discharging (see Fig. 1). Both conversions were modeled by the same efficiency (η_{ad}), which depends on a function of the input/output normalized power [36].

The HMG transfer function or BB model describes the development of the state variables derived from past states, control variables, and input disturbances. The BB energy at any time period j (Le^j_b) is computed in (18), considering the energy in the previous time period, self-discharge coefficient, energy exchange due to power-balance constraint, and the cumulated, stored, and released FCR energy:

$$Le^j_b = Le^{j-1}_b - \varepsilon_b \cdot Le^{j-1}_b + \Delta_t \cdot \left(\eta_{ad} \cdot \boldsymbol{p^j_{b-}} - \frac{\boldsymbol{p^j_{b+}}}{\eta_{ad}} \right) + \left(\eta_{ad} \cdot E^j_{\text{fcr}-} - \frac{E^j_{\text{fcr}+}}{\eta_{ad}} \right); \quad \forall j \tag{18}$$

According to requirements for FCR-units with limited energy reservoirs [89–93], these units need to be capable of providing the full prequalified FCR power for at least 30 min in the positive/negative direction (30-min criterion) during regular FCR operation. Consequently, the maximum BB energy for any time period j ($Le^{\max,j}_b$) is calculated by (18). However, it is necessary to take into account the maximum increase of stored FCR energy for the full prequalified FCR power activation (downward regulation):

$$Le^{\max,j}_b = Le^{j-1}_b - \varepsilon_{ub} \cdot Le^{j-1}_b + \Delta_t \cdot \left(\eta_{ad} \cdot \boldsymbol{p^j_{b-}} - \frac{\boldsymbol{p^j_{b+}}}{\eta_{ad}} \right) + \eta_{ad} \cdot \boldsymbol{\Omega_{ufcr}} \cdot P_{\text{ufcr}}; \quad \forall j \tag{19}$$

A similar equation is defined for the minimum BB energy (upward regulation):

$$Le^{\min,j}_b = Le^{j-1}_b - \varepsilon_{ub} \cdot Le^{j-1}_b + \Delta_t \cdot \left(\eta_{ad} \cdot \boldsymbol{p^j_{b-}} - \frac{\boldsymbol{p^j_{b+}}}{\eta_{ad}} \right) - \frac{\boldsymbol{\Omega_{ufcr}} \cdot P_{ufcr}}{\eta_{ad}}; \quad \forall j \tag{20}$$

4.6. Constraints

4.6.1. Constraints on sizing control variables

The constraints on the sizing control variables define the space that ensures that the HMG complies with a certain level of reliability. For the PV power, BB, and prequalified FCR power capacity, specific constraints are respectively:

$$0 \le \boldsymbol{\Omega_{upv}} \le \Omega^{\max}_{upv}$$
$$0 \le \boldsymbol{\Omega_{ub}} \le \Omega^{\max}_{ub}$$
$$0 \le \boldsymbol{\Omega_{upfc}} \le \Omega^{\max}_{upfc} \tag{21}$$

4.6.2. Power balance constraint

The total power balance condition is that the sum of all power exchanged through the AC link must be equal to zero. This includes the following types of power: (i) power bought from (and fed to) the grid; (ii) power obtained from (and injected into) the BB, considering the efficiency; (iii) power obtained from the PV system; (iv) power injected into the HLC, including the EVCL.

$$p^j_{g+} - p^j_{g-} + \boldsymbol{p^j_{b+}} - \boldsymbol{p^j_{b-}} + p^j_{pv} - p^j_{ev} - p^j_{hl} = 0; \quad \forall j \tag{22}$$

4.6.3. Battery constraints

Equation (23) limits the maximum power entering the BB, whereas (24) limits the maximum power coming out of it. Both are based on the maximum *C-rate:*

$$\boldsymbol{p^j_{b-}} + p^j_{pfc-} \le \boldsymbol{\Omega_{ub}} \cdot P^{\max}_{ub-}; \quad \forall j \tag{23}$$

$$\boldsymbol{p^j_{b+}} + p^j_{pfc+} \le \boldsymbol{\Omega_{ub}} \cdot P^{\max}_{ub+}; \quad \forall j \tag{24}$$

Equation (25) states the upper and lower bounds for the MBU energy. The lower bound is related to the rated DOD (χ^{rat}_{ub}). This was a set parameter in our formulation, which reduced computational complexity.

$$\boldsymbol{\Omega_{ub}} \cdot Le^{\max}_{ub} \left(1 - \frac{\chi^{rat}_{ub}}{100} \right) \le Le^j_b \le \boldsymbol{\Omega_{ub}} \cdot Le^{\max}_{ub}; \quad \forall j \tag{25}$$

within a 30-min criterion, (29) and (30) have the BB providing FCR between an upper and lower bound in order to cover the worst case scenario of the full activation of the prequalified FCR power for any time period *j*. This avoids long or short positions.

$$Le^{\max,j}_b \le \boldsymbol{\Omega_{ub}} \cdot Le^{\max}_{uB}; \quad \forall j \tag{26}$$

$$Le^{\min,j}_b \ge \boldsymbol{\Omega_{ub}} \cdot Le^{\max}_{ub} \left(1 - \frac{\chi^{ub}_{dod}}{100} \right) \quad \forall j \tag{27}$$

As formulated in equation (28), MBU energy at the beginning and end of optimization should be equal. The positivity of control and state variables is represented in (29).

$$Le^{beg}_{ub} = Le^{end}_{ub} \tag{28}$$

$$\boldsymbol{p^j_{b+}}, \boldsymbol{p^j_{b-}}, Le^j_b, \ Le^{\max,j}_b, \ Le^{\min,j}_b \ge 0 \quad \forall j \tag{29}$$

4.6.4. AC/DC converter constraints

Equations (30) and (31) state the power limit of the AC/DC converter. The number of MADUs should allow the power exchange of BB by means of the power balance constraint and FCR provision:

$$\boldsymbol{p^j_{b-}} + p^j_{pfc-} \le \Omega_{uad} \cdot P_{uad}; \quad \forall j \tag{30}$$

$$\boldsymbol{p^j_{b+}} + p^j_{pfc+} \le \Omega_{uad} \cdot P_{uad}; \quad \forall j \tag{31}$$

4.6.5. Grid power exchange constraints

The power exchanged between the HMG and LV AC grid at any

Please cite this article as: Gomez-Gonzalez M et al., Optimal sizing and power schedule in PV household-prosumers for improving PV self-consumption and providing frequency containment reserve, Energy, https://doi.org/10.1016/j.energy.2019.116554

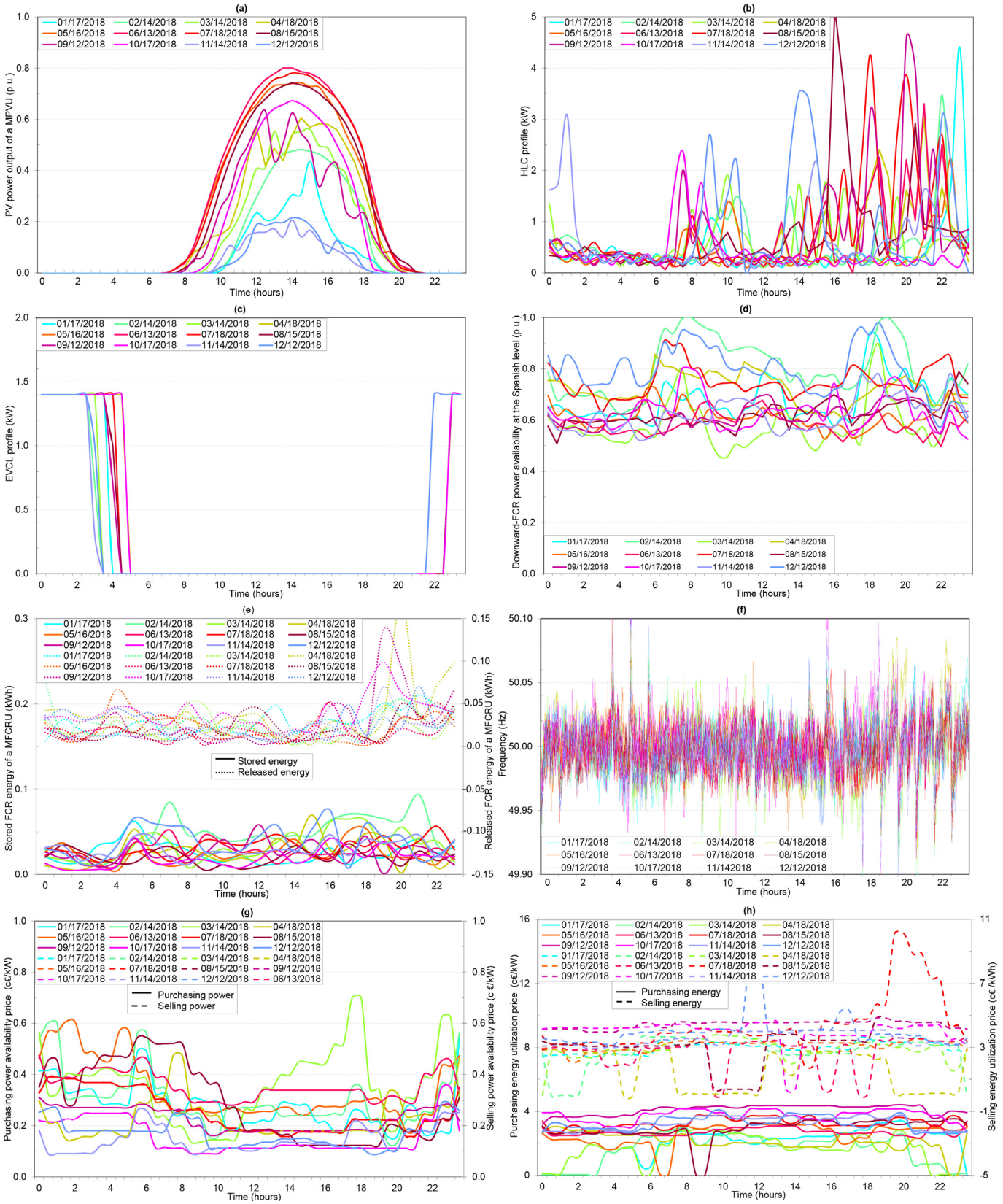

Fig. 3. The input data for one representative day of each month in 2018 (household #1): (a) PV power output of an MPVU; (b) HCL profile; (c) EVCL profile; (d) normalized data of downward FCR power availability at the Spanish level; (e) profile of cumulated stored, and released FCR energy of an MFCRU; (f) frequency profile at Hernani, Spain; (g) purchasing/selling power availability price; (h) purchasing/selling energy utilization price.

Please cite this article as: Gomez-Gonzalez M et al., Optimal sizing and power schedule in PV household-prosumers for improving PV self-consumption and providing frequency containment reserve, Energy, https://doi.org/10.1016/j.energy.2019.116554

Table 1
Key features of households in Jaen (southern Spain).

	Household #1	Household #2
Total annual consumption (kWh/year)	5731	5230
Number of family members	5	2
Is there at least one adult at home in the morning?	Yes	No
Electric heating	Yes	No
Building type	Apartment	Detached house

time period j is limited by the contracted power from electric mains:

$$p^j_{g+} + p^j_{\text{frc}-} \le P_c; \quad \forall j \tag{32}$$

$$p^j_{g-} + p^j_{\text{frc}+} \le P_c; \quad \forall j \tag{33}$$

5. Input data

This section describes the data for input disturbances at 30-min intervals.

5.1. PV power

Two PV power profiles were measured in two households at different locations in Jaen (southern Spain) with PV systems of 2.97 and 4.2 kWp. The annual final yields in 2018 were 1433 and 1411 kWh/kWp. To better compare the profiles, both were normalized to a 1400-kWh/kWp annual final yield. Fig. 3a shows the per-unit PV power output of an MPVU (ξ^j_{pv}) for one representative day of each month in household #1.

5.2. Household consumption load and EV charging load

The HLC (p^j_{hl}) and EVCL (p^j_{ev}) profiles (Fig. 3b and c) were measured by a smart meter [88] in these households. The profiles varied in regard to the relation between the peak and base load and load fluctuations. Table 1 shows their main features. To facilitate comparison, consumption profiles were normalized to a 5450-kWh annual electricity consumption (average Spanish-household energy [94,95]). The EV charging dataset was measured for the same households.

5.3. Data for FCR

New bids in the FCR service market from aggregators dealing with PV household-prosumers can alter the settlement of selected prices and bids. Nonetheless, even if these aggregators are a lower market fraction, the settlement will not substantially change. Since it is assumed that the aggregator is a price taker, this has no effect on market prices, which permitted data collection from current FCR markets.

Regarding FCR power availability, the technical requirements for the Spanish FCR market include a symmetry of the offer and a 1-h product resolution [96]. The hourly upward or downward regulation of FCR power availability at the Spanish level can be characterized by the per-unit downward and upward FCR power availability ($\xi^j_{\text{frc}-}$, $\xi^j_{\text{frc}+}$). Without knowing the outcome of new aggregator bids in the FCR market, it is assumed that the FCR power availability of a single PV household-prosumer in regard to its prequalified FCR power capacity will modulate in the same way as FCR power availability at the Spanish level. Fig. 3d depicts the normalized data of downward FCR power availability at the Spanish level ($\xi^j_{\text{frc}-}$) provided by the Spanish SO for one representative day of each month.

Regarding FCR energy utilization, Fig. 3e shows the cumulated stored and released FCR energy from an MFCRU (Section 4.4.1). As this energy depends on frequency deviation patterns, current frequency data from the UCTE in 2018 were used. Data were provided by the Spanish SO with a 50-Hz sampling rate at a specific point in the synchronous area of continental Europe (Hernani, Spain) (Fig. 3f).

Regarding FCR remuneration, since Spain does not regulate either FCR market or energy aggregation, this research used data from the European market (joint tender of German, Dutch, Belgian, Swiss, French, and Austrian SOs) [97]. In this area, payments are both for availability and utilization as well as for downward or upward regulation. Historic market data (FCR tendering results) of the year 2018 are displayed in Fig. 3g and h. As can be observed, the

Table 2
Technical and financial parameters applied in the optimization (first semester 2019) in Spain.

Parameter	Value	Parameter	Value	Parameter	Value
Δt	0.5 h	P^{uad}	1 kW/unit	$\Omega^{\max}_{upv}$	10 units
$\kappa_{pv}, \kappa_b, \kappa_{ad}$	1.5%, 2%, 0.3% [100]	$P^{\max}_{ub-}/P^{\max}_{ub+}$	1.0 kW (C-rate = 1)	$\Omega^{\max}_{upfc}$	5 units
d	3.5% [84]	P^{upv}	1 kWp/unit	$\Omega^{\max}_{ub}$	15 units
g	1.4% [101]	P_{ufcr}	0.5 kW/unit	$Le^{\max}_{ub}$	1 kWh (100%)
r_{pv}	0.5% [102,103]	Maximum prequalified power capacity for households	2.5 kW [19]	$Le^{beg}_{ub} = Le^{end}_{uB}$	0.65 kWh (65%)
$r_{O\&M}$ (= g)	1.4% of investment per year [2]	P_c	5 kW	χ^{rat}_{dod}	80% [45] unless otherwise stated
T	0% [2]	N_{uad}	20 years	Average life cycle (number of full cycles at 80% DOD	6400
C_{uad}	200 €/unit [45]	N_{ub}	20 years	Calendar lifetime	20 year [45]
C_{ub}	350 €/unit [31,32,45,84]	N_{upv}	20 years	MBU self-discharge coefficient	0.004%/day [45]
C_{upv}	1300 €/unit [45]	N_{hmg}	20 years		

Please cite this article as: Gomez-Gonzalez M et al., Optimal sizing and power schedule in PV household-prosumers for improving PV self-consumption and providing frequency containment reserve, Energy, https://doi.org/10.1016/j.energy.2019.116554

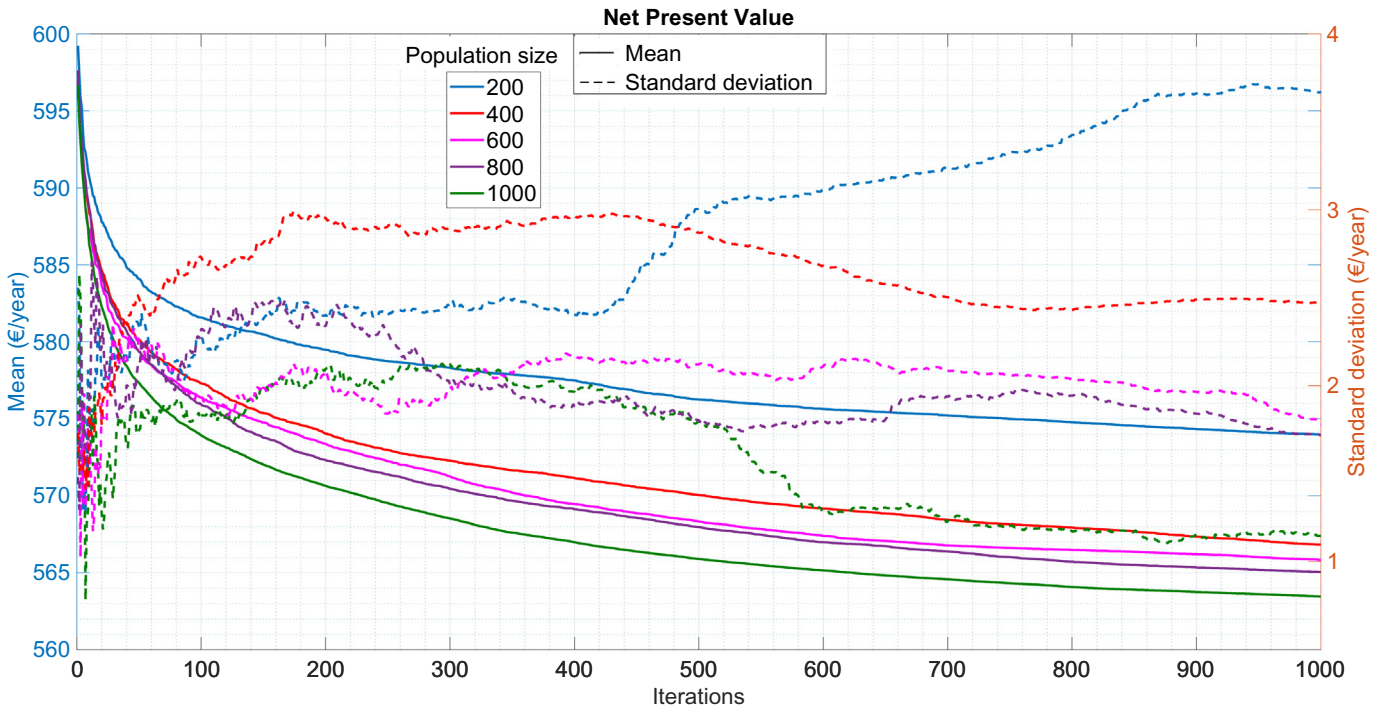

Fig. 4. Best solution for various population-size values.

power availability price significantly increased during nighttime hours, and especially in summer.

5.4. Energy price data

Our research study used Spanish real-time energy prices, which are publicly available on the website of the Iberian energy market [98].

6. Results

The two case studies validate the methodology presented in this study. The first case assessed the impact of various scenarios on the optimal sizing and power management of two PV household-prosumers by analyzing costs, revenues, and battery aging. Subsequently, for an illustrative scenario and prosumer, the second case focused on the parameter impact related to battery aging. The convergence of proposed optimization technique has been previously proven.

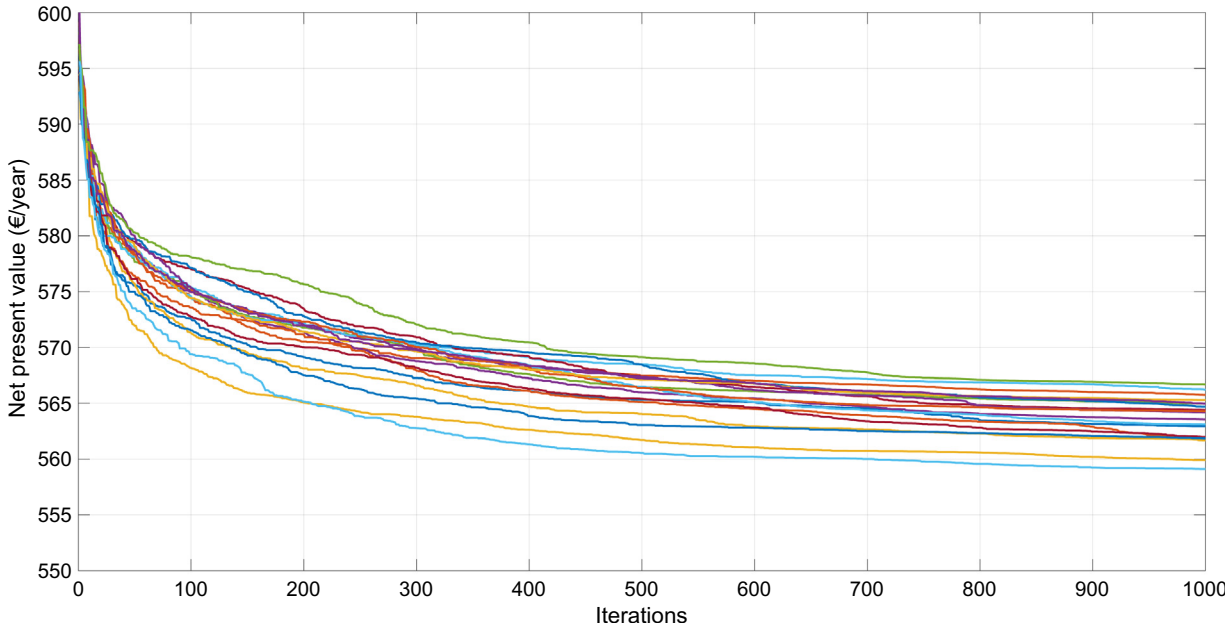

Fig. 5. Convergence of the optimization algorithm.

Please cite this article as: Gomez-Gonzalez M et al., Optimal sizing and power schedule in PV household-prosumers for improving PV self-consumption and providing frequency containment reserve, Energy, https://doi.org/10.1016/j.energy.2019.116554

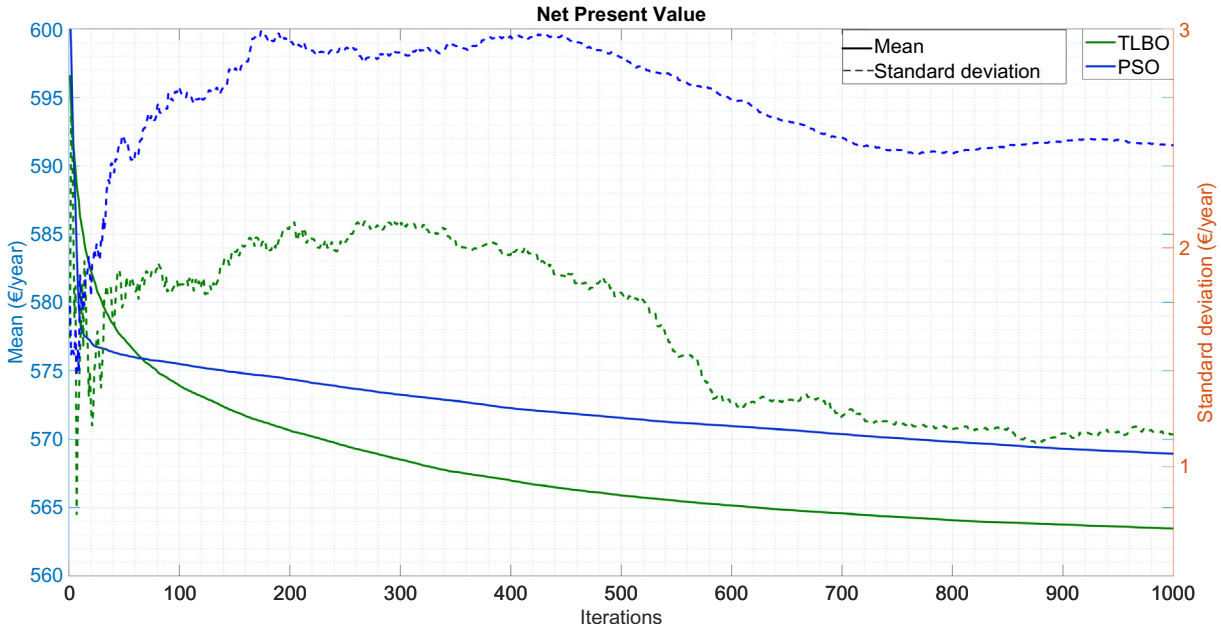

Fig. 6. Comparison with reference optimization algorithms.

The optimization problem in Section 4 was solved in the MATLAB programming environment. The computer used had a processor Intel® Core™ i7-8750H + HM370 (6 cores), 2.2–4.1 GHz, and 16-GB DDR4. To perform an accurate techno-economic assessment, the annual optimization problem included 4032 intervals of 0.5 h. This was based on 48 intervals of 0.5-h per day for seven days of each month.

The technical and financial parameters are listed in Table 2. The FMS parameters of the model for FCR provision were the same as those in the literature [18]. The battery aging parameters are those in Ref. [99].100101102103.

6.1. Accuracy and convergence of the optimization technique

The convergence of the TLBO algorithm was proved on the HMG with HLG, PV, and BB (hereafter defined as scenario #2). The number of iterations and the population were changed to determine optimization technique convergence. Each optimization was run 30 times, and resulted in the means and standard deviations in Fig. 4.

Fig. 5 shows the convergence curves of the TLBO algorithm for 20 independent runs of a population of 1000. The algorithm converged to the optimal fitness value after about 800 iterations. Therefore, 1000 iterations were considered as a fair termination criterion. From Figs. 4 and 5, we selected the following values: 1000 iterations and a population size of 1000 (about 0.0012% of the possible solution number).

Table 3
Solution report of the optimization problem for household #1.

	Variables	Constraints	Computational time (seconds)
Scenario #0A	–	–	<0.01
Scenario #0B	–	–	<0.01
Scenario #1	1	8065	22
Scenario #2	16128	20170	1922
Scenario #3	12096	20169	1337
Scenario #4	20160	20171	2710
Scenario #5	20160	20171	2763

Fig. 6 compares the convergence curves of the objective function for the TLBO algorithm as compared to the PSO algorithm (reference algorithm) after 30 runs and with the same computational effort. The TLBO algorithm was found to be more robust and efficient since it produced better results. Although the PSO algorithm was able to converge to obtain solutions of equal quality, it was necessary to increase the particle number and/or iterations. It thus had a higher computational cost.

6.2. Optimal sizing and power management of a PV household-prosumer in different scenarios

This section applies the methodology for jointly optimizing the sizing and power management of two PV household-prosumers in scenarios such as the following:

- Scenario #0A: base scenario with HCL.
- Scenario #0B: base scenario with HCL and EVCL.
- Scenario #1: scenario with HCL and PV (PV self-consumption).
- Scenario #2: scenario with HCL, PV, and BB (PV self-consumption enhancement). BB power management is scheduled.
- Scenario #3: scenario with a BB and FCR (FCR provision). Consumer offers FCR and BB power management is scheduled.
- Scenario #4: scenario with HCL, PV, BB, and FCR (PV self-consumption enhancement plus FCR provision).
- Scenario #5: scenario #4 plus EVCL.

The summary of the optimization problem for household #1 is given in Table 3. As can be observed, the computational load rapidly (and critically) increases with the number of planned time periods and control variables.

In order to investigate the impact of these scenarios, the first results presented are those regarding the optimal power management at the optimal HMG sizing for household #1. The second group of results pertains to optimal sizing, battery aging, and economic issues. Finally, a comparison of optimal sizing results for household #2 is provided.

Figs. 7–11 show the optimal power schedule for household

Please cite this article as: Gomez-Gonzalez M et al., Optimal sizing and power schedule in PV household-prosumers for improving PV self-consumption and providing frequency containment reserve, Energy, https://doi.org/10.1016/j.energy.2019.116554

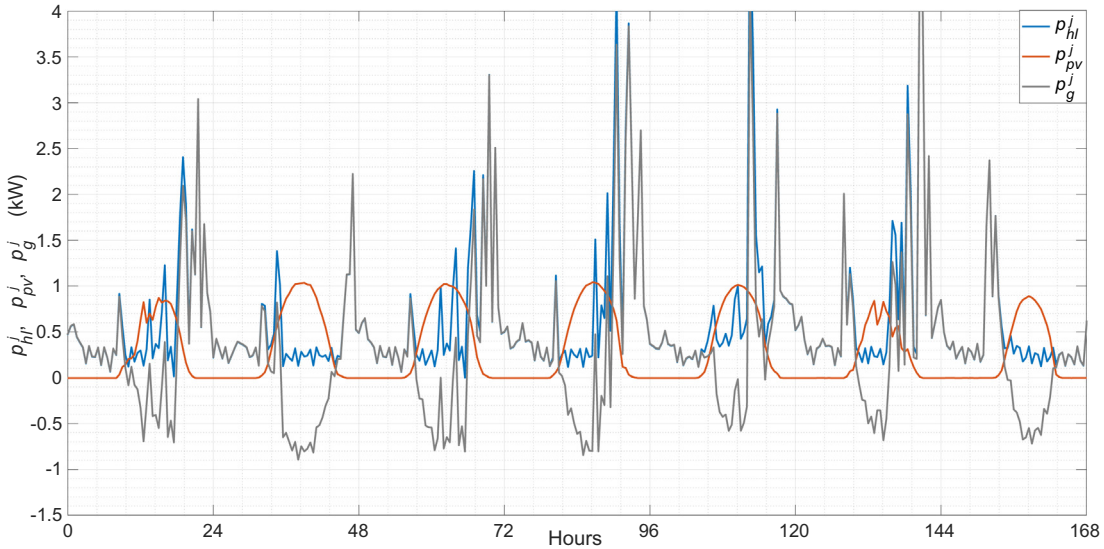

Fig. 7. Scenario #1 (HCL and PV), 7 days starting from May 15, 2018 (household #1): optimal power schedule at the optimal HMG sizing.

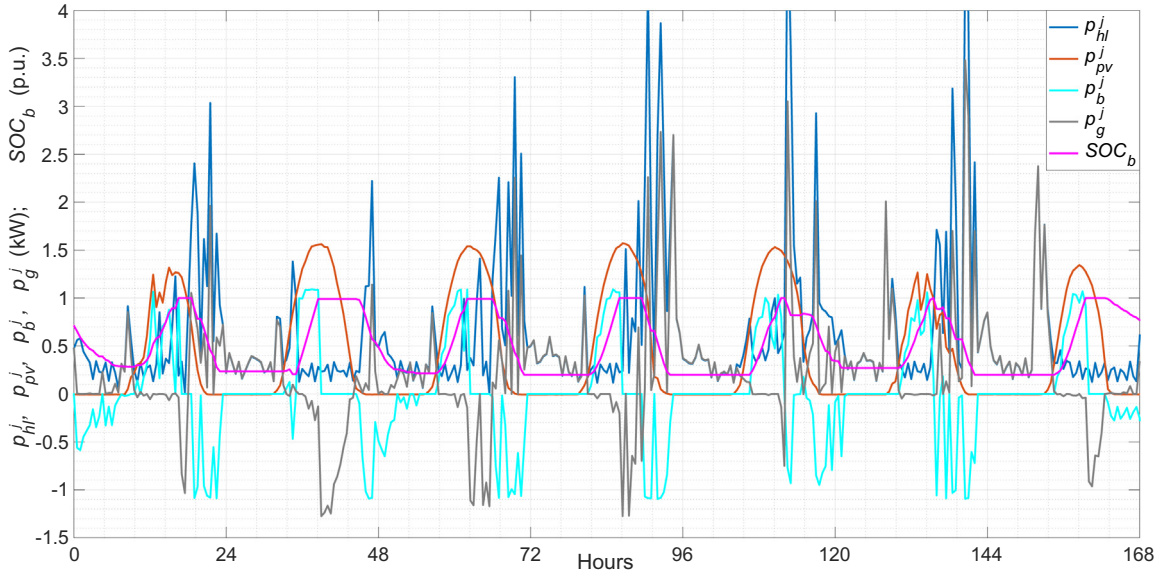

Fig. 8. Scenario #2 (HCL, PV, and BB), household #1: optimal power schedule at the optimal HMG sizing.

#1 at the optimal HMG sizing over a period of 7 days, starting from May 15, 2018. From 9 a.m. to 11 a.m., there was surplus PV power, as shown in scenarios #1, #2, #4, and #5. However, the surplus PV generation was not sold back to the grid (as occurred in scenario #1 [$p^j_g < 0$ (p^j_{g-})] during this period) because the real-time energy price was not high enough. Instead, it was stored in the BB. Then, when this price rose to a certain threshold value, the peak HCL demand (scenarios #2 and #4) and EVCL demand (scenario #5) were provided by means of BB discharging. Interestingly, for scenario #2, the BB gradually charged in the first half of each day until it was at its full capacity, and then gradually discharged in the second half until it was empty. However, in scenarios #4 and #5, the larger BB sizing, required for providing FCR, together with a more continuous power requirement, smoothed SOC variation of the BB.

Fig. 9 focuses on the FCR provision, i.e., scenario #3. The SOC fluctuations of the BB in micro and macro cycles reached a minimum value of 51.8% and a maximum of 67.8%. This signified that the BB did not effectively use its asset. Throughout the year (Table 4), it reached a minimum SOC of 51.5%, a mean value of 60.2%, and a maximum of 68.0%. Thus, the SOC fluctuated within the permitted bandwidth (i.e., a lower bound of 51.5% and an upper bound of 68.5%), which ensured the provision of full prequalified FCR power with a 30-min criterion. Furthermore, as SOC fluctuation was mostly within the previous range, this caused moderate calendar aging.

Figs. 10 and 11 show an almost unappreciable BB SOC change from the FCR provision that was so clearly visible in Fig. 9. This was due to shallow cycling, which had almost no effect on the macro cycles and accumulated energy throughput, and thus on the SOC of the larger BB. As can be observed, in both scenarios, the charge/discharge power schedule of the BB was different from scenario #2, which had a lower BB capacity even though the annual NPVs were equivalent. The implication is that the optimal BB power schedule is not necessarily unique. The strong temporal nonalignment of HLC

Please cite this article as: Gomez-Gonzalez M et al., Optimal sizing and power schedule in PV household-prosumers for improving PV self-consumption and providing frequency containment reserve, Energy, https://doi.org/10.1016/j.energy.2019.116554

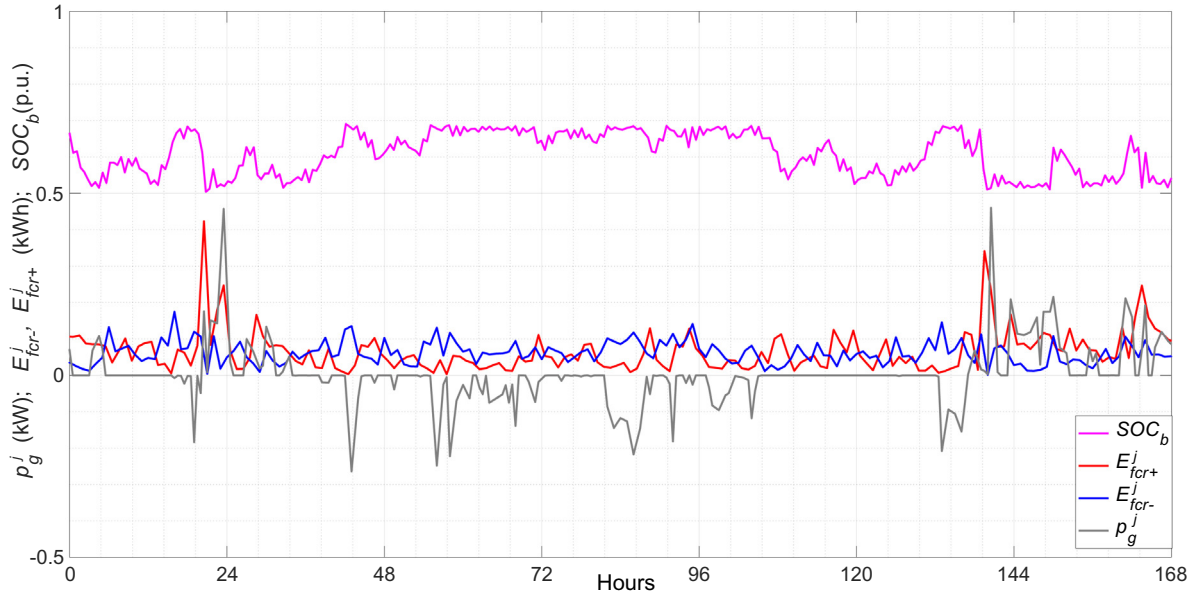

Fig. 9. Scenario #3 (BB and FCR), (household #1: optimal power and FCR energy schedule at the optimal HMG sizing.

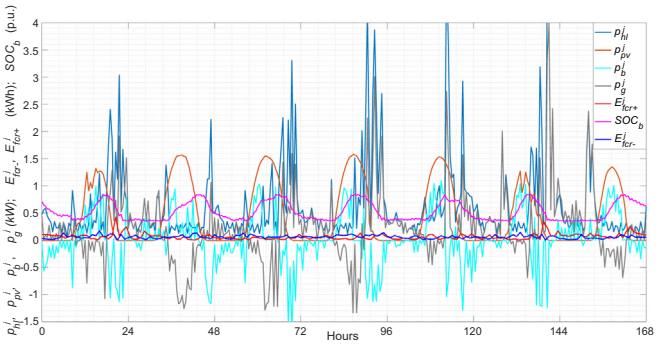

Fig. 10. Scenario #4 (HCL, PV, BB, and FCR), household #1: optimal power and FCR energy schedule at the optimal HMG sizing.

and high FCR availability prices could be a cause of this.

Fig. 12 shows the FCR provision results in terms of cumulated stored and released FCR energy, and energy exchanged with the LV grid by the BB power schedule. In scenario #3, the share of stored FCR energy accounted for up to 79.59% of the total amount of BB energy charging. The share of released FCR energy amounted to 86.22% of the total amount of BB energy discharging. In contrast, in scenarios #4 and #5, the FCR provision represented [2] no more than 38.92% and 28.26%, respectively, of the total amount of the energy exchange. The impact on aging must be low as they corresponded to an extremely small DOD [104].

Table 4 summarizes the results of optimal HMG sizing for household #1, including battery aging and economic issues. As for economic issues, the annual NPVs of all of the scenarios were within a profitable range in comparison to the base scenario (#0A or #0B). Scenario #1 was the starting point for the economic evaluation (i.e., the household use of PV electricity or PV self-consumption). This reduced the annual NPV from 663.05 to 599.29 €/year. In scenario #2, the BB power schedule for enhancing PV self-consumption offered an additional revenue stream of 33.02 €/year. Although thanks to FCR, scenario #3 showed promising results because there was a return, the economic incentive of 16.18 €/year was relatively small.

Nonetheless, the profitability of providing FCR changed considerably in scenarios that had PV self-consumption enhancement, either with HCL (scenario #4) or with EVCL (scenario #5). Thus, an additional revenue of 76.57 €/year was achieved in scenario #4 in comparison to scenario #2. The poor economic result of scenario #3 compared to scenarios #4 or #5 was due to the BB, which had to maintain a high reserve level in order to comply with the 30-min criterion. The results indicated that scenarios #4 and #5 were the best options.

When profitability was also evaluated by the LCOE, single PV self-consumption decreased the LCOE by 9.6%. The PV self-consumption enhancement reduced it additionally by 5.5%, and finally the joint practice of also providing FCR produced an even greater reduction of 13.5%. When the EVCL was involved, a 19.6% total enhancement was achieved.

In scenarios #2, #4, and #5, the optimal sizing of PV power varied slightly from 2.00 to 2.46 kWp. In contrast, because of the 30-min criterion, there was an extra sizing in scenarios #4 and #5 (7.97–9.92 kWh) in comparison to scenario #2 (4.74 kWh). However, this extra sizing was lower than required when there was only FCR provision (scenario #3). When the BB sizing was larger, there was greater flexibility in the use of the BB by different applications since it could be used as needed. In addition, more energy could be stored for larger PV power sizing. The maximum sizing values for scenario #5 were the result of the higher mixed load (i.e. HCL plus EVCL). Finally, scenario #2 had the lowest PV power sizing (1.375 kWp) in order to avoid surplus PV generation sold back to the grid.

BB lifetime expectancies were sensitive to planned scenarios and thus differed significantly. The BB reached a cycling lifetime of 18.05 years in scenario #2, and 29.73 and 26.68 years in scenarios #4 and #5, respectively. Cycling lifetime increased to 88.76 years in scenario #3. The shallow cycling characteristic of the latter scenario made calendar aging predominant. In contrast, BB aging behavior changed for the alternative practice of PV self-consumption enhancement (scenario #2). This practice, along with greater depths of discharge (e.g. daily cycling) would lead to different cyclic aging during several weeks per year and therefore influence the overall expected lifetime. As a result, the joint practice of PV self-consumption enhancement and FCR provision (scenarios #4 and

Please cite this article as: Gomez-Gonzalez M et al., Optimal sizing and power schedule in PV household-prosumers for improving PV self-consumption and providing frequency containment reserve, Energy, https://doi.org/10.1016/j.energy.2019.116554

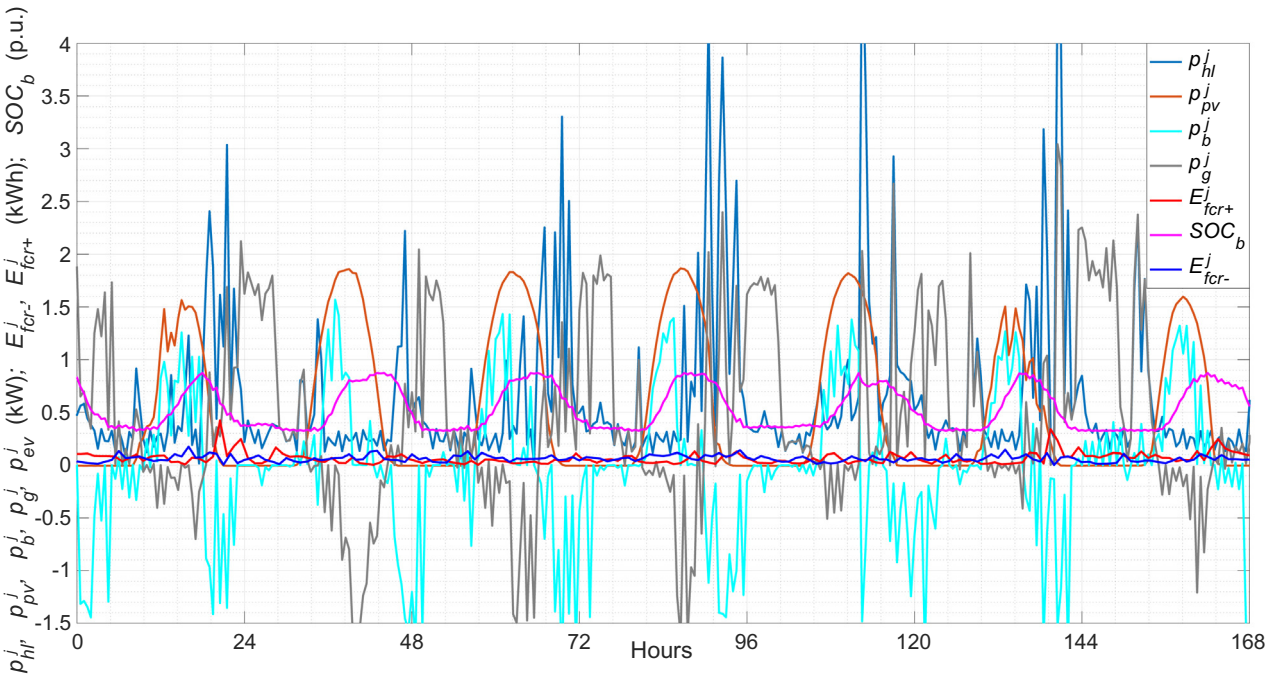

Fig. 11. Scenario #5 (scenario #4 plus EVCL), household #1: optimal power and FCR energy schedule at the optimal sizing.

Table 4
Summary of optimal economic and sizing results for household #1.

Scenario	Annual NPV (€/year)	LCOE (€/kWh)	PV system (kWp)	AC/DC converter (kW)	Prequalified power capacity household (kW)	BB (kWh)	Minimum SOC of BB (%)	Maximum SOC of BB (%)	Cycling lifetime (years)	Calendar lifetime (years)	DOD (%)
#0A	663.05	0.12166	0.000	0.000	0.0	0.00	–	–	–	–	
#0B	966.12	0.11700	0.000	0.000	0.0	0.00	–	–	–	–	
#1	599.29	0.10996	1.375	0.000	0.0	0.00	–	–	–	–	
#2	566.26	0.10390	2.000	1.094	0.0	4.74	20.0	100.0	18.05	20	80
#3	−16.18	−0.00297	0.000	3.008	2.5	3.96	51.5	68.0	88.76	20	80
#4	489.70	0.08985	2.083	2.982	2.5	7.97	35.7	84.0	29.73	20	80
#5	775.84	0.09396	2.468	3.242	2.5	9.92	32.6	87.0	26.68	20	80

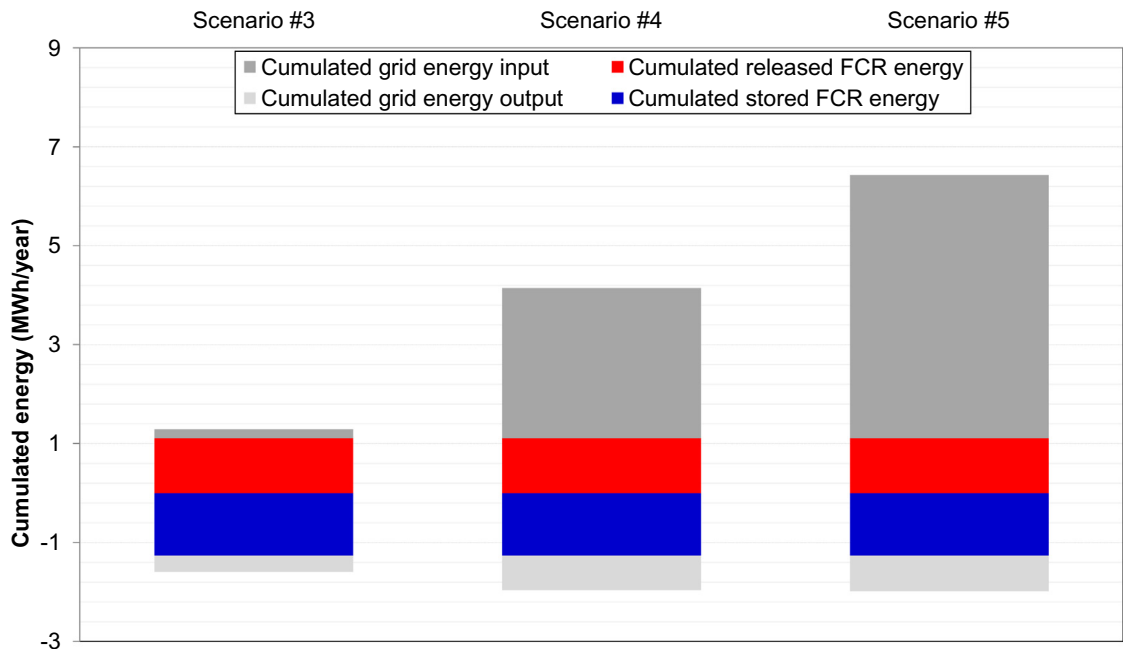

Fig. 12. Annual amount of energy exchanged through FCR provision and energy exchanged with the LV grid.

Please cite this article as: Gomez-Gonzalez M et al., Optimal sizing and power schedule in PV household-prosumers for improving PV self-consumption and providing frequency containment reserve, Energy, https://doi.org/10.1016/j.energy.2019.116554

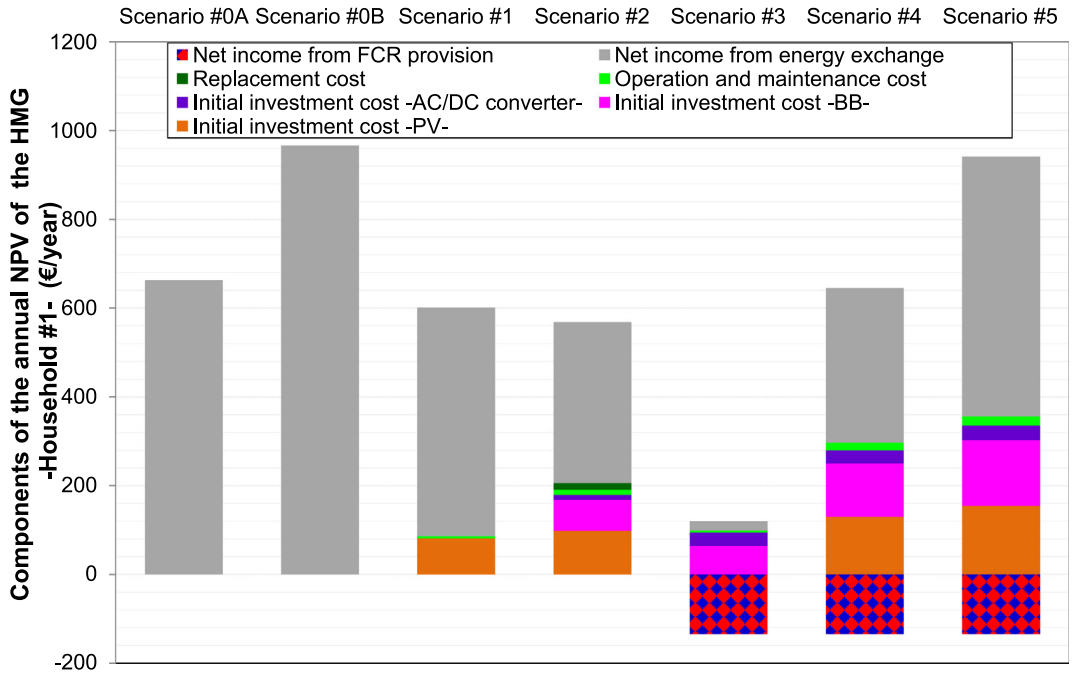

Fig. 13. Composition of incomes and costs as part of the annual NPV for household #1.

Table 5
FCR economic analysis for household #1.

	Net income for aggregator (€/year)	Net income for prosumer (€/year)	Prosumer's gains for FCR power availability (€/year)	Prosumer's gains for FCR energy utilization (€/year)
Scenarios #3, #4, and #5	172.55	134.32	56.66	77.65

Table 6
Summary of the optimal economic and sizing results for household #2.

Scenario	Annual NPV (€/year)	LCOE (€/kWh)	PV system (kWp)	AC/DC converter (kW)	Prequalified power capacity household (kW)	BB (kWh)	Minimum SOC of BB (%)	Maximum SOC of BB (%)	Cycling lifetime (years)	Calendar lifetime (years)	DOD (%)
#0A	644.81	0.11831	0.000	0.000	0.0	0.00	–	–	–	–	80
#0B	947.87	0.11479	0.000	0.000	0.0	0.00	–	–	–	–	80
#1	550.97	0.10110	1.859	0.000	0.0	0.00	–	–	–	–	80
#2	523.36	0.09603	1.968	1.251	0.0	4.48	0.200	1.00	18.35	20	80
#3	−16.19	−0.00297	0.000	3.008	2.5	3.96	0.515	0.68	88.76	20	80
#4	450.18	0.08260	1.937	2.743	2.5	6.78	0.384	0.82	34.65	20	80
#5	744.52	0.09016	2.248	2.995	2.5	8.32	0.350	0.85	31.60	20	80

Table 7
Summary of the optimal economic and sizing results for household #1 in scenario #2: several DODs.

Annual NPV (€/year)	LCOE (€/kWh)	PV system (kWp)	AC/DC converter (kW)	BB (kWh)	Minimum SOC of BB (%)	Maximum SOC of BB (%)	Cycling lifetime (years)	Calendar lifetime (years)	DOD (%)
566.26	0.10390	2.000	1.094	4.74	20.0	100	18.05	20	80
594.51	0.10908	1.682	0.964	1.81	40	100	25.41	20	60
598.56	0.10983	1.387	0.142	0.14	50	100	18.71	20	50
598.78	0.10987	1.451	0.087	0.11	60	100	27.75	20	40
599.29	0.10996	1.375	0.000	0.00	80	100	99.63	20	20

#5) showed a mixed aging behavior. Only scenario #2 required a BB replacement in the 17th year of operation.

For a better understanding of the contribution of each economic component to the annual NPV, the incomes and costs described in Section 4.3 are presented as part of the whole NPV for household #1 in different scenarios (see Fig. 13).

As can be observed in scenario #1, in comparison to #0A, the additional initial PV investment cost was clearly compensated by

Please cite this article as: Gomez-Gonzalez M et al., Optimal sizing and power schedule in PV household-prosumers for improving PV self-consumption and providing frequency containment reserve, Energy, https://doi.org/10.1016/j.energy.2019.116554

the additional revenues from the lower energy exchange. The economic enhancement in scenario #2, compared to scenario #1, largely stemmed from a reduction in the net income of energy exchange because of the optimal BB power schedule in spite of the higher initial investment cost. The economic feasibility of only providing FCR (scenario #3) was largely influenced by the initial investment costs. Thus, the cost of the energy exchange to maintain the energy level of the BB within the limits required by the 30-min criterion was only 20.38%. The economic analysis in Table 5 revealed that payments for FCR energy utilization represented more than 59% of the income. This shows how the economic enhancement in scenario #4, as compared to scenario #2, was the result of both the enhancement of PV self-consumption (lower energy exchange) and FCR provision, despite the higher initial investment cost. This also occurred with greater intensity in scenario #5, compared to scenario #0B, because of the higher energy load. Therefore, the optimal sizing favors the hybrid solution of providing FCR and PV self-consumption enhancement.

In order to compare the optimal HMG sizing in household #2 with different profiles, the results of this methodology are given in Table 6. In scenario #0A, the HCL in household #1 resulted in a higher annual NPV and LCOE (even though the normalized load was the same as household #2) because the peak of the load coincided with a higher real-time energy price. In scenario #1, the best profile matching (load-PV generation) in household #2 favored increasing PV power. In scenario #2, the HCL in household #1 resulted in more optimal BB sizing, presumably because the peak load occurred during the peak pricing period and reductions in surplus PV production had to be balanced by additional BB capacity. The same outcome can be seen in scenarios #4 and #5.

6.3. Impact of parameters related with battery aging

A sensitivity analysis was performed to identify the lowest annual NPV related to the allowed DOD in the BB for household #1 in scenario #2. For this purpose, the DOD value was changed to 20%, 40%, 50%, 60%, and 80%. The other parameters remained constant. Table 7 summarizes the economic results. More specifically, these pertain to the optimal annual NPV and LCOE as well as the optimal HMG sizing results. The cycling lifetime of the BB is also provided.

As can be observed, the lower DOD values offer the lowest BB sizing and cost savings. The lower DOD involves a higher number of cycles and an increase in the battery cycling lifetime. As a result, it was possible to plan a lower BB sizing, which had the advantage of maintaining battery cycling lifetime and decreasing costs. However, this lower BB sizing made it more difficult to enhance PV self-consumption, which reduced PV system sizing. The lowest simulated DOD (20%) devised an HMG without a BB. Therefore, for this scenario with daily macro cycles, it is important to plan a large DOD in order to obtain the full storage capacity of the right BB sizing for PV self-consumption enhancement.

7. Conclusions

The main objective of this research was to demonstrate that there are interesting markets (balancing services market and day-ahead electricity market) for improving the profitability of PV household-prosumers. In contrast to previous approaches applied on residential PV-battery system optimization, this improvement could be achieved by jointly co-optimizing the sizing and power management of these PV household-prosumers. For this purpose, an innovative optimization methodology was developed. This methodology was implemented in the design of a model that quantified the total costs and revenues by means of an annual techno-economic assessment, which took into account a set of representative days. The costs and revenues included investment, operation and maintenance, replacement, net income from the energy exchange and the FCR provision. The model also made it possible to assess battery aging, depending on use. The TLBO algorithm was proposed as a technique to solve the optimization problem. Although the methodology focused on a case study based on Spanish PV household-prosumers, it can be applied to most market setups that have a liberalized market for energy and frequency reserve products.

The added value of this methodology was its flexibility in terms of solution accuracy and computational burden. Our research thus demonstrated how optimal results could be speedily and accurately obtained. This is very important not only for our study but also for further research focusing on shortening the simulation step with high-resolution inputs.

The optimization in various scenarios highlighted the fact that the income and savings obtained, thanks to the incorporation of PV, BB, and FCR provision were higher than the amortization costs. In general, PV self-consumption and profitability were greatly enhanced. Furthermore, the study proved the economic feasibility of providing only FCR through BBs. Nonetheless, the profitability of this provision considerably increased in scenarios with PV self-consumption enhancement. This made it possible to decrease the ratio of useable BB capacity, required by the 30-min criterion, which led to significant economic benefits because of reduced investment costs. These results confirmed the value of exploiting the inherent flexibility of BBs for providing mixed services.

BB aging evidently plays a crucial role in the final profitability because of the replacement cost. It was also found that FCR provision together with PV self-consumption enhancement significantly reduced BB costs because of a reduction of aging per kWh delivered. This was due to the lower impact of the shallow DOD cycles of the FCR provision.

As reflected in this study, the casuistry of the optimal sizing and power management in different scenarios and types of PV household-prosumers was quite varied. Regarding PV self-consumption enhancement, the optimal PV sizing could significantly range in both households from 1.37 to 2.00 kWp. In contrast, the quantitative relation between the BB capacity and PV power presented in this paper underlined a low BB sizing change of approximately 2.27–2.37 kWh/kWp. When this enhancement was combined with FCR provision, BB sizing was in the range 3.50–3.82 kWh/kWp only with HLC (3.70–4.01 kWh/kWp when EVCL was added). The two optimal capacity ranges were found to be different from one another because of the extra sizing needed to fulfill the 30-min criterion. In any case, lower BB values were observed for household #2 because of the best load-PV matching.

Future work in the field should take current weaknesses that the modelling of PV household-prosumer faces into consideration. It should thus focus on building a techno-economic system modelling which includes a hybrid ESS, which would be tested in real-world scenarios by decreasing the simulation step from input time series sampled at higher frequencies. This would permit an accurate evaluation of the battery degradation in hybrid ESSs and its technical and economic impact.

Acknowledgements

This research was funded by the Agencia Estatal de Investigación, Spain (AEI) and the Fondo Europeo de Desarrollo Regional (FEDER) aimed at the Challenges of Society (Grant No. ENE 2017-83860-R "Nuevos servicios de red para microredes renovables inteligentes. Contribución a la generación distribuida residencial").

Please cite this article as: Gomez-Gonzalez M et al., Optimal sizing and power schedule in PV household-prosumers for improving PV self-consumption and providing frequency containment reserve, Energy, https://doi.org/10.1016/j.energy.2019.116554

Appendix A. TLBO algorithm

Of the most commonly used optimization techniques [105,106], the most applicable to our research context are the following: (i) iterative and probabilistic approaches [56,61]; (ii) analytical methods [53,62]; (iii) directed search-based methods, such as those based mathematical optimization (e.g. mixed-integer linear programming [16,37,54,61,66], dynamic programming [64,67], and the design space based approach [60]) or heuristic methods (e.g. neural networks [59]). Of the population-based heuristic algorithms, the two most important groups are evolutionary algorithms [58] (e.g. genetic algorithm [59,65] and simulated annealing [57]) and swarm intelligence-based algorithms (e.g. particle swarm optimization (PSO) [55,56,63]).

All the population-based heuristic algorithms require common controlling parameters such as population size, number of generations, etc., as well as their own algorithm-specific control parameters that need to be tuned since these parameters affect their performance. Improper tuning either increases the computational effort or yields the local optimal solution. For this reason, reference [107] introduced the TLBO algorithm, which does not require any algorithm-specific parameters. The TLBO algorithm only requires common controlling parameters such as population size and number of generations for it to work satisfactorily.

The TLBO algorithm [108,109] is a teaching-learning process-inspired algorithm and is based on the effect of the influence of a teacher on the output of learners in a class. The algorithm describes two basic modes of learning: (i) through the teacher (teacher phase); and (ii) through interaction with the other learners (learner phase). In this optimization algorithm, a group of learners is considered to be a population and different subjects offered to the learners are regarded as different design variables of the optimization problem. A learner's result is analogous to the 'fitness' value of the optimization problem. The best solution in the entire population is considered to be the teacher.

Appendix B. Battery lifetime modelling

Modelling the battery lifetime is a field of ongoing research [99,110–113]. The main models are post-processing models and performance degradation [110]. Post-processing models include Ah-throughput models, which simply count the amount of charge until a fixed limit. In contrast, cycle-counting models [112] (e.g. Rainflow based on Downing's algorithm [113]) are based on counting the charge/discharge cycles corresponding to each DOD range for a year. Performance degradation models (e.g. weighted Ah-throughput model [113]) track the battery capacity reduction based on its actual operating condition.

The model of a battery lifespan (i.e. maximum number of battery cycles) is usually based on the charge/discharge power rate and DOD. The DOD at each cycle is obtained in our research from the BB SOC using the Rain Flow method [113]. The lifespan of a minimum battery unit (MBU) for a given specific discharge cycle m depends on the discharge power rate and DOD [99]:

$$\lambda_{ub,m}^{\max}\left(\boldsymbol{p}_{\boldsymbol{b}-}^{\boldsymbol{j}}, p_{pfc-}^{j}, DoD\right) = \frac{a_1 \cdot DoD_m^{a_2}}{\left(\frac{\boldsymbol{p}_{\boldsymbol{b}-}^{\boldsymbol{j}} + p_{pfc-}^{j}}{\boldsymbol{\Omega}_{\boldsymbol{ub}} \cdot Le_{ub}^{\max}}\right)^{a_3}} \tag{34}$$

The quantity of life consumed or aging rate of MBU for a given discharge cycle m is thus the following:

$$\theta_{ub,m} = \frac{1}{\lambda_{ub,m}^{\max}\left(\boldsymbol{p}_{\boldsymbol{b}-}^{\boldsymbol{j}}, p_{pfc-}^{j}, DoD\right)} \tag{35}$$

Consequently, the total fraction of life consumed or cumulated aging rate during the whole time horizon (θ_{ub}) can be obtained by adding the respective fractions of life consumed over all of the discharge cycles N_c :

$$\theta_{ub} = \sum_{m=1}^{m=N_c} \theta_{ub,m} \tag{36}$$

References

[1] Luthander R, Widen J, Nilsson D, Palm J. Photovoltaic self-consumption in buildings: a review. Appl Energy 2015;142:80–94.
[2] Talavera DL, Munoz-Rodriguez FJ, Jimenez-Castillo G, Rus-Casas C. A new approach to sizing the photovoltaic generator in self-consumption systems based on cost-competitiveness, maximizing direct self-consumption. Renew Energy 2019;130:1021–35.
[3] Schopfer S, Tiefenbeck V, Staake T. Economic assessment of photovoltaic battery systems based on household load profiles. Appl Energy 2018;223:229–48.
[4] Kaschu T, Jochem P, Fichtner W. Solar energy storage in German households: profitability, load changes and flexibility. Energy Policy 2016;98:520–32.
[5] Linssen J, Stenzel P, Fleer J. Techno-economic analysis of photovoltaic battery systems and the influence of different consumer load profiles. Appl Energy 2017;18:2019–25.
[6] Wolisz H, Schütz T, Blanke T, et al. Cost optimal sizing of smart buildings' energy system components considering changing end-consumer electricity markets. Energy 2017;137:715–28.
[7] Ngoc An L, Quoc-Tuan T, Seddik B, Van-Linh N. Optimal sizing of a grid-connected microgrid. In: Proc IEEE international conference on industrial technology (ICIT); 2015. p. 1–6. Seville (Spain).
[8] Bianchi M, Branchini L, Ferrari C, Melino F. Optimal sizing of grid-independent hybrid photovoltaic–battery power systems for household sector. Appl Energy 2014;136:805–16.
[9] Ru Y, Kleissl J, Martinez S. Storage size determination for grid-connected photovoltaic systems. IEEE Trans Sustain Energy 2013;4(1):68–81.
[10] Li J, Xue Y, Tian L, Yuan X. Research on optimal configuration strategy of energy storage capacity in grid connected microgrid. Prot Control Modern Power Syst 2017;2(35):1–7.
[11] Sevilla FRS, Knazkins V, Park C, Korba P. Advanced control of energy storage systems for pv installation maximizing self-consumption. IFAC-PapersOnLine 2015;48(30):524–8.
[12] Schlund J, German R. A control algorithm for a heterogeneous virtual battery storage providing FCR power. In: Proc IEEE international conference on smart grid and smart cities. Singapore: ICSGSC); 2017. p. 61–6.
[13] Megel O, Mathieu J, Andersson G. Scheduling distributed energy storage units to provide multiple service. In: Proc power systems computation conference (PSCC); 2014. p. 1–7. Wroclaw (Poland).
[14] Steber D, Bazan P, German R. SWARM - strategies for providing frequency containment reserve power with a distributed battery storage system. In: Proc IEEE international energy conference (ENERGYCON); 2016. p. 1–6. Leuven (Belgium).
[15] Litjens GBMA, Worrell E, van Sark WGJHM. Economic benefits of combining self-consumption enhancement with frequency restoration reserves provision by photovoltaic- battery systems. Appl Energy 2018;223:172–87.
[16] Kusakana K. Impact of different South African demand sectors on grid-connected PV systems' optimal energy dispatch under time of use tariff. Sustainable Energy Technol Assess 2018;27:150–8.
[17] Yang Y, Blaabjerg F, Wang H, et al. Power control flexibilities for grid-connected multi-functional photovoltaic inverters. IET Renew Power Gener 2016;10(4):504–13.
[18] Hernández JC, Bueno PG, Sanchez-Sutil F. Enhanced utility-scale PV units with frequency support functions and dynamic grid support for transmission systems. IET Renew Power Gener 2017;11(3):361–72.
[19] Hernández JC, Sanchez-Sutil F, Vidal PG, Rus-Casas C. Primary frequency control and dynamic grid support for vehicle-to-grid in transmission systems. Int J Electr Power Energy Syst 2018;100:152–66.
[20] Greenwood DM, Lim KY, Patsios C, Lyons PF, Lim YS, Taylora PC. Frequency response services designed for energy storage. Appl Energy 2017;203:115–27.
[21] CENELEC TS 50549-2. Requirements for generating plants to be connected in parallel with distribution networks: connection to a MV distribution network above 16 A. 2015.
[22] IEC 0-16. Reference technical rules for the connection of active and passive consumers to the HV and MV electrical networks of distribution company.

Please cite this article as: Gomez-Gonzalez M et al., Optimal sizing and power schedule in PV household-prosumers for improving PV self-consumption and providing frequency containment reserve, Energy, https://doi.org/10.1016/j.energy.2019.116554

2014.
[23] German TSOs. Anforderungen an die Speicherkapazität bei batterien für die primärregelleistung. German Transmission System Operators: 50Hertz, Amprion, Tennet. Transnet BW; 2015.
[24] German TSOs. Eckpunkte und freiheitsgrade bei erbringung von primärregelleistung. Leitfaden für anbieter von primärregelleistung. German Transmission System Operators: 50Hertz, Amprion, Tennet. Transnet BW; 2014.
[25] CENELEC TS 50549-1. Requirements for generating plants to be connected in parallel with distribution networks: connection to a LV distribution network above 16 A. 2015.
[26] IEC 0-21. Reference technical rules for the connection of active and passive users to the LV electrical utilities. 2014.
[27] CENELEC EN 50438. Requirements for micro-generating plants to be connected in parallel with public LV distribution networks. 2013.
[28] Calderaro V, Galdi V, Lamberti F, et al. A smart strategy for voltage control ancillary service in distribution networks. IEEE Trans Power Syst 2015;30:494–502.
[29] Roos M, Holthuizen B. Congestion of LV distribution networks by household battery energy storage systems utilized for FCR, aFRR and market trading. In: Proc 53rd International Universities Power Engineering Conference (UPEC); 2018. p. 1–6. Glasgow (Scotland).
[30] Bampoulas A, Karlis A. Provision of frequency regulation by a residential microgrid integrating PVs, energy storage and electric vehicle. In: Proc IEEE international conference on environment and electrical engineering and IEEE industrial and commercial power systems Europe (EEEIC/I&CPS Europe); 2017. p. 1–6. Milan (Italy).
[31] Canals Casals L, Barbero M, Corchero C. Reused second life batteries for aggregated demand response services. J Clean Prod 2019;212:99–108.
[32] Melo SP, Brand U, Vogt T, Telle JS, Schuldt F, Maydell KV. Primary frequency control provided by hybrid battery storage and power-to-heat system. Appl Energy 2019;233/234:220–31.
[33] German TSOs. Internet platform for control reserve tendering. https://www.regelleistung.net/. [Accessed 26 June 2019].
[34] Dunn B, Kamath H, Tarascon JM. Electrical energy storage for the grid: a battery of choices. Science 2011;334:928–35.
[35] Reinier AC, van der Veen, Hakvoort RA. The electricity balancing market: exploring the design challenge. Util Policy 2016;43(B):186–94.
[36] SEDC. Explicit demand response in Europe Mapping the markets. 2017.
[37] Rezaei N, Kalantar M. Smart microgrid hierarchical frequency control ancillary service provision based on virtual inertia concept: an integrated demand response and droop controlled distributed generation framework. Energy Convers Manag 2015;92:287–301.
[38] Fini MH, Golshan MEH. Frequency control using loads and generators capacity in power systems with a high penetration of renewables. Electr Power Syst Res 2019;166:43–51.
[39] Braun M, Strauss P. A review on aggregation approaches of controllable distributed energy units in electrical power systems. Int J Distrib Energy Resour 2008;4:297–319.
[40] Olivella-Rosell P, Bullich-Massagu E, Aragües-Peñalba M, et al. Optimization problem for meeting distribution system operator requests in local flexibility markets with distributed energy resources. Appl Energy 2018;210:881–95.
[41] Teng F, Mu Y, Jia H, Wu J, Zeng P, Strbac G. Challenges on primary frequency control and potential solution from EVs in the future GB electricity system. Appl Energy 2017;194:353–62.
[42] Kempton W, Tomic J, Letendre S, Brooks A, Lipman T. Vehicle-to-grid power: battery, hybrid, and fuel cell vehicles as resources for distributed electric power in California. June 2001. UCD-ITS-RR-01-03.
[43] Borsche T, Ulbig A, Koller M, Andersson G. Power and energy capacity requirements of storages providing frequency control reserves. In: Proc IEEE power energy society general meeting; 2013. p. 1–5. Vancouver (Canada).
[44] Hollinger R, Diazgranados LM, Erge T. Trends in the German PCR market: perspectives for battery systems. In: Proc 15th international conference on the European energy market (EEM); 2015. p. 1–6. Lodz (Poland).
[45] Lombardi P, Schwabe F. Sharing economy as a new business model for energy storage systems. Appl Energy 2017;188:485–96.
[46] Johnston L, Díaz-González F, Gomis-Bellmunt O, Corchero-García C, Cruz-Zambrano M. Methodology for the economic optimisation of energy storage systems for frequency support in wind power plants. Appl Energy 2015;137:660–9.
[47] Oudalov A, Chartouni D, Ohler C. Optimizing a battery energy storage system for primary frequency control. IEEE Trans Power Syst 2007;22(3):1259–66.
[48] Fleer J, Stenzel P. Impact analysis of different operation strategies for battery energy storage systems providing primary control reserve. J Energy Storage 2016;72(2015):19.
[49] Fleer J, Zurmühlen S, Badeda J, Stenzel P, Hake JF, Sauer DU. Model-based economic assessment of stationary battery systems providing primary control reserve. Energy Procedia 2016;99:11–24.
[50] Swierczynski M, Stroe DI, Stan AI, Teodorescu R. Primary frequency regulation with Li-ion battery energy storage system: a case study for Denmark. In: Proc 5th IEEE Annual International Energy Conversion Congress and Exhibition (ECCE); 2013. p. 1–6. Melbourne (Australia).
[51] Swierczynski M, Stroe DI, Stan AI, Teodorescu R, Sauer DU. Selection and performance-degradation modeling of LiMO2/Li4Ti5O12 and LiFePO4/C battery cells as suitable energy storage systems for grid integration with wind power plants: an example for the primary frequency regulation service. IEEE Trans Sustainable Energy2014;5(1):90–101.
[52] Sánchez V, Ramirez JM, Arriaga G. Optimal sizing of a hybrid renewable system. In: Proc IEEE international conference on industrial technology; 2010. p. 1–6. Vina del Mar (Chile).
[53] Wang XY, Mahinda Vilathgamuwa D, Choi SS. Determination of battery storage capacity in energy buffer for wind farm. IEEE Trans Energy Convers 2008;23(3):868–78.
[54] Bahramirad S, Reder W, Khodaei A. Reliability-constrained optimal sizing of energy storage system in a microgrid. IEEE Trans Smart Grid 2012;3(4):2056–62.
[55] Kashefi A, Kaviani Riahy GH, Kouhsari SHM. Optimal design of a reliable hydrogen-based stand-alone wind/PV generating system, considering component outages. Renew Energy 2009;34(11):2380–90.
[56] Valizadeh Haghi H, Hakimi SM, Moghaddas Tafreshi SM. Optimal sizing of a hybrid power system considering wind power uncertainty using PSO-embedded stochastic simulation. In: Proc 11th IEEE international conference on probabilistic methods applied to power systems; 2010. p. 1–6 (United States).
[57] Ekrena O, Ekrenb BY. Size optimization of a PV/wind hybrid energy conversion system with battery storage using simulated annealing. Appl Energy 2010;87(2):592–8.
[58] Bernal-Agustín JL, Dufo-López R. Efficient design of hybrid renewable energy systems using evolutionary algorithms. Energy Convers Manag 2009;50(3):479–89.
[59] Mellita A, Kalogirou SA, Drif M. Application of neural networks and genetic algorithms for sizing of photovoltaic systems. Renew Energy 2010;35(12):2881–93.
[60] Muselli M, Notton G, Louche A. Design of hybrid-photovoltaic power generator, with optimization of energy management. Sol Energy 1999;65(3):143–57.
[61] Fazlalipour P, Ehsan M, Mohammadi-Ivatloo B. Optimal participation of low voltage renewable micro-grids in energy and spinning reserve markets under price uncertainties International. Int J Electr Power Energy Syst 2018;102:84–96.
[62] Mercier P, Cherkaoui R, Oudalov A. Optimizing a battery energy storage system for frequency control application in an isolated power system. IEEE Trans Power Syst 2009;24(3):1469–77.
[63] Shanga C, Srinivasan D, Reindl T. An improved particle swarm optimisation algorithm applied to battery sizing for stand-alone hybrid power systems. Int J Electr Power Energy Syst 2016;74:104–17.
[64] Nguyen TA, Crow ML, Elmore AC. Optimal sizing of a vanadium redox battery system for microgrid systems. IEEE Trans Sustain Energy 2015;6(3):729–37.
[65] Fossati JP, Galarza A, Martín-Villate A, Fontán L. A method for optimal sizing energy storage systems for microgrids. Renew Energy 2015;77:539–49.
[66] Dargahi A, Ploix S, Soroudi A, Wurtz F. Optimal household energy management using V2H flexibilities. Int J Computations Math Electr 2014;33(3):777–93.
[67] Liu Y, Yuen C, Ul Hassan N, Huang S, Yu R, Xie S. Electricity cost minimization for a microgrid with distributed energy resource under different information availability. IEEE Trans Ind Electron 2015;62(4):2571–83.
[68] Battke B, Schmidt TS. Cost-efficient demand-pull policies for multi-purpose technologies – the case of stationary electricity storage. Appl Energy 2015;155:334–48.
[69] Fleer J, Zurmühlen S, Meyer J, Badeda J, Stenzel P, Hake J-F, Sauer DU. Techno-economic evaluation of battery energy storage systems on the primary control reserve market under consideration of price trends and bidding strategies. J Energy Storage 2018;17:345–56.
[70] Hernandez JC, Sanchez-Sutil F, Muñoz-Rodríguez FJ. Design criteria for the optimal sizing of a hybrid energy storage system in PV household-prosumers to maximize self-consumption and self-sufficiency. Energy 2019;186:115827.
[71] Parsopoulos KE, Vrahatis MN. On the computation of all global minimizers through particle swarm optimization. IEEE Trans Evol Comput June 2004;8(3):211–24.
[72] Ardakani FJ, Riahy G, Abedi M. Design of an optimum hybrid renewable energy system considering reliability indices. In: Proc 18th Iranian conference on electrical engineering (ICEE); 2010. p. 842–7. Isfahan (Iran).
[73] Thompson AW. Economic implications of lithium ion battery degradation for Vehicle-to-Grid (V2X) services. J Power Sources 2018;396:691–709.
[74] Persson M. Frequency response by wind farms in power systems with high wind power penetration. Thesis at Department of Electrical Engineering. Gothenburg, Sweden: Chalmers University of Technology; 2017.
[75] ENTSO-E. Entso-e network code on electricity balancing. 2014., version 3.0.
[76] ENTSO-E. Electricity balancing network code. Commission Regulation (EU) 2017/2195 of 23 November 2017 establishing a guideline on electricity balancing. 2017. Article 2(6), Article 14(1), Article 16, Article 18(4), (5), (7), Article 43.
[77] ENTSO-E. Network code on load-frequency control and reserves. 2013.
[78] ENTSO-E. Operational reserve ad hoc team report. 2012.
[79] ENTSO-E. Supporting document for the network code on electricity balancing of 23 December 2013 and the amended version of 6 August 2014. 2014.
[80] Rebours YG, Kirschen DS, Trotignon M, Rossignol S. A Survey of frequency and voltage control ancillary services-Part I: technical features. IEEE Trans Power Syst 2007;22(1):350–7.

Please cite this article as: Gomez-Gonzalez M et al., Optimal sizing and power schedule in PV household-prosumers for improving PV self-consumption and providing frequency containment reserve, Energy, https://doi.org/10.1016/j.energy.2019.116554

[81] Tendayi Mandi tereza P, Bansal R. Renewable distributed generation: the hidden challenges – a review from the protection perspective. Renew Sustain Energy Rev 2016;58:1457–65.
[82] Lai CS, McCulloch MD. Levelized cost of energy for PV and grid scale energy storage systems. Appl Energy 2016:1–11.
[83] Bendato I, Bonfiglio A, Brignone M, et al. Design criteria for the optimal sizing of integrated photovoltaic-storage systems. Energy 2018;149:505–15.
[84] United Nations Environment Programme (UNEP). Bloomberg new energy finance (BNEF). http://www.iberglobal.com/files/2018/renewable_trends.pdf. [Accessed 26 June 2019].
[85] ENTSO-E. Network code on electricity balancing. A EURELECTRIC comments paper. August 2013. p. 1.
[86] ENTSO-E. A1-Appendix 1: load-frequency control and performance, continental Europe Operation handbook european network of transmission system operators for electricity (ENTSO-E).
[87] ENTSO-E. Network code on requirements for grid connection applicable to all generators. 2015.
[88] Hernandez JC, Ruiz-Rodriguez FJ, Jurado F. Modelling and assessment of the combined technical impact of electric vehicles and photovoltaic generation in radial distribution systems. Energy 2017;141:316–32.
[89] Tech. Rep. Anforderungen an die Speicherkapazität bei batterien fr die primärregelleistung regelleistung.net. September 2015. https://www.regelleistung.netlextldownload/anforderungBatterien. [Accessed 26 June 2019].
[90] ENTSO-E. Explanation of FCR energy requirement for CE and NE as defined in NC. LFCR; 2013.
[91] Red Eléctrica de España. Technical guidelines draft for wind and photovoltaic power plants connected directly to the distribution and transmission network: minimum requirements of design, equipment, operation, setting in service and security. Spain. 2014 [in Spanish)].
[92] ACER and European network of transmission system operators for electricity. European Commission: System operation guideline draft; 2015.
[93] German Transmission System Operators (TSOs). Anforderungen an die Speicherkapazität bei Batterien für die Primärregelleistung. 2015.
[94] National institute of statistics of Spain. http://www.ine.es. [Accessed 26 June 2019].
[95] Eurostat. Electricity consumption by households. http://ec.europa.eu/eurostat. [Accessed 26 June 2019].
[96] Red eléctrica de España. https://www.ree.es/es. [Accessed 26 June 2019].
[97] RegelleistungNet. Internetplattform zur Vergabe von Regelleistung. https://www.regelleistung.net/apps/datacenter/tenders/?productTypes=PRL,SRL,MRL&from=2019-07-02&to=2019-07-09&tid=PRL_20190702_D1. [Accessed 3 July 2019].
[98] Mercado ibérico de Energía (OMIE). http://www.omel.es/inicio. [Accessed 26 June 2019].
[99] de la Torre S, González-González JM, Aguado JA, Martín S. Optimal battery sizing considering degradation for renewable energy integration. IET Renew Power Gener 2019;13(4):572–7.
[100] Breyer C, Gerlach A. Global overview on grid-parity. Prog Photovolt Res Appl 2013;21:121–36.
[101] Trading Economics. Inflation rate countries list. http://www.tradingeconomics.com/country-list/inflation-rate. [Accessed 26 June 2019].
[102] Jordan DC, Kurtz SR. Photovoltaic degradation rates - an analytical review. Prog Photovolt Res Appl 2013;21:12–29.
[103] Branker K, Pathak MJM, Pearce JM. A review of solar photovoltaic levelized cost of electricity. Renew Sustain Energy Rev 2011;15:4470–82.
[104] Warnecke A. Ageing effects of Lithium-ion batteries. In: Proc 17th conference on power electronics and applications; 2015. p. 1–20. Geneva (Switzerland).
[105] Erdinc O, Uzunoglu M. Optimum design of hybrid renewable energy systems: overview of different approaches. Renew Sustain Energy Rev 2012;16(3):1412–25.
[106] Yang Y, Bremner S, Menictas C, Kay M. Battery energy storage system size determination in renewable energy systems: a review. Renew Sustain Energy Rev 2018;9:109–25.
[107] Rao RV, Savsani VJ, Vakharia DP. Teaching–learning-based optimization: a novel method for constrained mechanical design optimization problems. Comput Aided Des 2011;43(3):303–15.
[108] Rao RV, Savsani VJ, Vakharia DP. Teaching-learning-based optimization: an optimization method for continuous non-linear large scale problems. Inf Sci 2012;183(1):1–15.
[109] Rao RV. Review of applications of TLBO algorithm and a tutorial for beginners to solve the unconstrained and constrained optimization problems. Decision Science Letters 2016;5:1–30.
[110] Dufo-Lopez R, Lujano-Rojas JM, Bernal-Agustín JL. Comparison of different lead-acid battery lifetime prediction models for use simulation of stand-alone PV systems. Appl Energy 2014;115:242–53.
[111] Omar N, Monem MA, Firouz Y, et al. Lithium iron phosphate based battery. Assessment of the aging parameters and development of cycle life model. Appl Energy 2014;113:1575–85.
[112] Musallam M, Johnson CM. An efficient implementation of the Rainflow counting algorithm for life consumption estimation. IEEE Trans Reliab 2012;61(4). 978–968.
[113] Downing SD, Socie DF. Simple rainflow counting algorithms. Int J Fatigue 1982;4:31–40.

Please cite this article as: Gomez-Gonzalez M et al., Optimal sizing and power schedule in PV household-prosumers for improving PV self-consumption and providing frequency containment reserve, Energy, https://doi.org/10.1016/j.energy.2019.116554